2017-11-01

# Developing New Classes of Thick-Origami-Based Mechanisms: Conceal-and-Reveal Motion and Folding Printed Circuit Boards

Bryce Parker De Figueiredo
*Brigham Young University*

# Developing New Classes of Thick-Origami-Based Mechanisms: Conceal-and-Reveal Motion and Folding Printed Circuit Boards

Bryce Parker DeFigueiredo

A thesis submitted to the faculty of
Brigham Young University
in partial fulfillment of the requirements for the degree of

Master of Science

Larry L. Howell, Chair
Spencer P. Magleby
Christopher A. Mattson

Department of Mechanical Engineering

Brigham Young University

ABSTRACT

Developing New Classes of Thick-Origami-Based Mechanisms: Conceal-and-Reveal Motion and Folding Printed Circuit Boards

Bryce Parker DeFigueiredo
Department of Mechanical Engineering, BYU
Master of Science

Origami-adapted mechanisms form the basis of an increasing number of engineered systems. As most of these systems require the use of non-paper materials, various methods for accommodating thickness have been developed. These methods have opened new avenues for origami-based design. This work introduces approaches for the design of two new classes of thick-origami systems and demonstrates the approaches in hardware. One type of system, called "conceal-and-reveal," is introduced, and a method of designing these mechanisms is developed. Techniques are also developed for designing folding printed circuit boards which are fabricated from a single sheet of material. This enables areas of regional flexibility, leaving other areas stiff. This allows components to be attached to stiff regions and folding to occur at flexible regions. An optimization method is presented to design the geometry of surrogate hinges to aid in monolithic origami-based mechanisms such as flexible PCBs. Examples are shown which demonstrate each of these new techniques.

Keywords: Origami, Compliant Mechanisms, Surrogate Hinges

# ACKNOWLEDGMENTS

I would like to thank my colleagues in the Compliant Mechanisms Research Group for their help in developing the research this thesis is based on. Mike Morgan, Erica Crampton, Kyler Tolman, Bryce Barker, Nathan Pehrson, Trent Zimmerman, and Brian Russell contributed significantly to the ideas, designs, and prototypes presented here. Jason Allen and Jason Lund also helped in developing the models used in the design and analysis. Thanks to Hannah Lutz as well for developing beautiful concept illustrations used in this research.

I would like to express further appreciation to my graduate committee members, Dr. Larry Howell, Dr. Spencer Magleby, and Dr. Chris Mattson for their expertise and guidance in my research. I want to thank them for the impact they have had on my career and personal development. Their mentorship has truly changed the trajectory of my life.

Finally, I would like to thank my family for their love and support, which has enabled me to get to this point. My parents Denis and Sharon DeFigueiredo supported, inspired, and encouraged me to pursue my education to the fullest. My wife Kate has provided an unending amount of love and patience on this journey.

This work is based on research supported by funding from the National Science Foundation and the Air Force Office of Scientific Research under Grant No. 1240417. Any opinions, findings, and conclusions or recommendations expressed in this thesis are those of the authors and do not necessarily reflect the views of the National Science Foundation.

TABLE OF CONTENTS

**LIST OF TABLES** . . . . . **vi**

**LIST OF FIGURES** . . . . . **vii**

**Chapter 1 Introduction** . . . . . **1**
1.1 Background: Origami in Engineering Design . . . . . 1
1.2 New Avenues for Origami Design: Conceal-and-Reveal Mechanisms . . . . . 2
1.3 Origami Electronics: Regional Stiffness Reduction for Printed Circuit Board Design 2
1.4 Computational Method for Optimization of Surrogate Hinges in Origami Design . 3
1.5 Research Objectives . . . . . 3

**Chapter 2 Origami-based Design of Conceal-and-Reveal Systems** . . . . . **4**
2.1 Introduction . . . . . 4
2.2 Background . . . . . 5
2.2.1 Origami in Engineering Design . . . . . 5
2.2.2 Rigid Origami and Thick Origami . . . . . 5
2.2.3 Design Process . . . . . 7
2.3 Conceal-and-Reveal Motion . . . . . 7
2.4 Method . . . . . 8
2.4.1 Define Problem . . . . . 8
2.4.2 Select Origami Pattern . . . . . 8
2.4.3 Modify and Refine Origami Pattern . . . . . 10
2.4.4 Select Thickness-Accommodation Method . . . . . 11
2.4.5 Modify for Application-Specific Elements . . . . . 11
2.4.6 Modify for Manufacturing . . . . . 12
2.5 Examples . . . . . 12
2.5.1 Problem Definition . . . . . 12
2.6 Example 1: Square Twist Array . . . . . 13
2.6.1 Origami Pattern Selection . . . . . 13
2.6.2 Pattern Modification . . . . . 13
2.6.3 Thickness Accommodation . . . . . 14
2.6.4 Payload Accommodation . . . . . 16
2.6.5 Modification for Manufacturing . . . . . 16
2.7 Example 2: Modified Hexagon Twist . . . . . 17
2.7.1 Origami Pattern Selection . . . . . 17
2.7.2 Pattern Modification . . . . . 17
2.7.3 Thickness Accommodation . . . . . 17
2.7.4 Payload Accommodation . . . . . 18
2.7.5 Modification for Manufacturing . . . . . 19
2.8 Example 3: Chicken Wire Tessellation . . . . . 22
2.8.1 Origami Pattern Selection . . . . . 23
2.8.2 Pattern Modification . . . . . 23

2.8.3 Thickness Accommodation . . . 24
2.8.4 Payload Accommodation . . . 25
2.8.5 Modification for Manufacturing . . . 25
2.9 Conclusion . . . 26

**Chapter 3 Regional Stiffness Reduction Using Lamina Emergent Torsional Joints for Flexible Printed Circuit Board Design . . . 28**
3.1 Introduction . . . 28
3.2 Background . . . 29
3.2.1 Flexible Electronics . . . 29
3.2.2 Surrogate Hinges . . . 30
3.3 Approach . . . 30
3.3.1 Models and Analysis . . . 31
3.3.2 Prototype Design . . . 36
3.3.3 Testing . . . 38
3.3.4 Origami Map Fold . . . 39
3.4 Conclusion . . . 41

**Chapter 4 Optimization of LET Joint Arrays for Use as Surrogate Hinges in Monolithic Thick Origami . . . 46**
4.1 Introduction . . . 46
4.2 Background . . . 46
4.3 Approach . . . 47
4.3.1 Constants . . . 47
4.3.2 Variables . . . 48
4.3.3 Equations . . . 49
4.3.4 Objective Function and Constraints . . . 52
4.4 Results . . . 53
4.5 Conclusion . . . 55

**Chapter 5 Conclusion . . . 56**
5.1 Summary . . . 56
5.2 Limitations . . . 56
5.3 Conclusions . . . 57
5.4 Future Work . . . 58

**REFERENCES . . . 60**

LIST OF TABLES

3.1 Comparison of analytical and finite element model results. The Von Mises stress is listed, based on a 180° angular displacement load. Note that $m$ is the number of LET joints in parallel and $n$ is the number of LET joints in series (see Fig. 3.5). . . . . 36
3.2 Resistance measurements of each trace on two boards before and after 100,000 cycles of 180 degree deflection. All values are in Ω. The small changes in resistance show that no mechanical failure occurred over the duration of the fatigue test. . . . . 40

4.1 Constants in LET joint array optimization. . . . . 48
4.2 LET joint array design variables to be optimized. . . . . 50
4.3 Results from the LET joint array parameter optimization. $\alpha$, $\beta$, and $\gamma$ correspond to the surrogate hinges in Fig. 4.2. Columns labeled "Opt." correspond to optimization results. Columns labeled "Fab." correspond to the modified structure that was fabricated. Fabricated dimensions differ from optimized dimensions to facilitate the entire structure fitting in the given area. . . . . 54

LIST OF FIGURES

2.1 Thick-origami mechanisms and rigid-origami mechanisms are subsets of origami-adapted mechanisms. . . . . 6
2.2 This chart introduces a process for designing thick, rigid-origami mechanisms. It is applied to produce origami mechanisms that exhibit conceal-and-reveal motion. . . . . 9
2.3 Square twist origami pattern modified for conceal-and-reveal behavior. (a) Original square twist fold pattern. Blue solid lines represent mountain folds, and red dashed lines represent valley folds. (b) Four arrayed square twists. This is the intermediate step to get from the square twist on the left to the modified pattern on the right. (c) Modified square twist pattern. The grey area indicates the portion used in this mechanism. . . . . 14
2.4 An illustration of the revealed (left) and concealed (right) configurations of the arrayed square-twist pattern. Colors represent different layers in the closed configuration and correspond to the colors in Fig. 2.5. . . . . 15
2.5 A CAD model of the Square Twist Array attached to an open box. The colors of the panels correspond to the colors in Fig. 2.4. . . . . 15
2.6 Section view of the payload and lift mechanism of the Square Twist Array. The yellow block represents the payload. When the panels open and close, the black strip translates their motion to lift the payload up and down. . . . . 16
2.7 Prototype of Square Twist Array conceal-and-reveal mechanism. . . . . 17
2.8 Modification of the hexagonal twist pattern. (a) Original hexagon twist pattern. Blue solid lines represent mountain folds, and red dashed lines represent valley folds. (b) Modification of exterior panels for conceal and reveal motion. (c) Modification of pattern for thickness accommodation using Axis Shift technique. . . . . 18
2.9 Modified Hexagon Twist with thick panels going through its folding motion. . . . . 19
2.10 Linkages for actuation. (a) Sarrus linkages (red) lift the payload as the panels open. (b) Links behind mechanism panels couple the motion of the panels with the motion of the lid. . . . . 20
2.11 Sarrus mechanism (red) used in the actuation of the Modified Hexagon Array. . . . . 20
2.12 Four-bar mechanism (red) formed by links coupling the motion of the origami array with the lid. Images show mechanism starting (a) fully open and (b,c) going through closing motion. . . . . 21
2.13 A compression spring (red) assists with the actuation of the Modified Hexagon Array. . 22
2.14 Prototype of Modified Hexagon Twist conceal-and-reveal mechanism. . . . . 22
2.15 Chicken Wire Tessellation origami pattern. Blue solid lines represent mountain folds, and red dashed lines represent valley folds. . . . . 23
2.16 Chicken Wire Tessellation folding into a pseudo-cylindrical concave shell. Note that further motion is prevented by self-intersection. The pattern is modified to avoid this, as shown in Fig. 2.17. . . . . 24
2.17 Modification of the Chicken Wire Tessellation Pattern. Panels labeled with X's are removed, and gray panels are added. . . . . 24
2.18 Parallelogram linkage (red) used to lift the payload out of storage for the Chicken Wire Tessellation conceal-and-reveal box. . . . . 25

2.19 A prototype of the Chicken Wire Tessellation conceal-and-reveal mechanism. . . . . 26

3.1 Current techniques for producing flexible electronics allow for uncontrolled deflection of the entire substrate. When the circuit is (a) undeflected, components and solder joints experience low stresses. When the circuit is (b) deflected, components and solder joints experience high stresses. . . . . 30
3.2 (a) A single LET joint and (b) an array of LET joints. LET joint geometry lowers stiffness by transferring an applied bending load over the joint to torsional loads in the legs. . . . . 31
3.3 (a) A single LET joint with its corresponding spring system and (b) geometric parameters for Eq. 3.1-3.12. . . . . 32
3.4 Deflected LET joint with parameters from Eq. 3.1 labeled. . . . . 33
3.5 Detail view of LET joint array. . . . . 35
3.6 (a) Prototype solar array with LET joint hinge in folded and (b) unfolded configurations, along with (c) a detail view of the LET joint array surrogate hinge. . . . . 37
3.7 (a) Diagram and (b) photograph of fatigue testing setup. . . . . 39
3.8 Map-fold origami pattern. (a) Origami fold pattern. Blue solid lines represent mountain folds, and red dashed lines represent valley folds. Labels A, B, and C designate the three folding steps in order of folding sequence. (b) The fold area to be made flexible with surrogate hinges is shown shaded in green. (c) Surrogate hinge areas are colored. Red arrows show the direction of the fold axis. Labels $\alpha$, $\beta$, and $\gamma$ designate regions of optimized surrogate fold geometry. Gray regions show areas where material is removed. 43
3.9 Origami-like folding structure designed with optimized surrogate hinge LET joint arrays and fabricated from a single sheet of copper-clad FR-4. . . . . 44
3.10 Possible form factors for various applications of this regional stiffness reduction technique. Circuit boards could be folded to stow in small spaces or to conform to an arbitrary shape. . . . . 45

4.1 LET joint array with design variables labeled. . . . . 49
4.2 Monolithic map fold origami structure from Sec. 3.3.4. Regions $\alpha$, $\beta$, and $\gamma$ were optimized separately. . . . . 53

# CHAPTER 1. INTRODUCTION

## 1.1 Background: Origami in Engineering Design

Origami is a centuries-old art form that is increasingly being used by engineers in mechanical design. Traditionally, origami involves folding a single square piece of paper with no cuts. As engineers have moved towards using origami as a design paradigm to make useful products, they have confronted challenges in adapting origami principles to applications requiring robust materials. This research addresses challenges with using thick materials in origami-based design and develops ways to adapt origami to solve engineering design problems.

One hurdle to overcome is adapting paper origami patterns to applications requiring materials that are thicker and stiffer than paper. Paper origami is approximated using zero-thickness models with creases that act as ideal hinges. This means that an origami model consists of two-dimensional planar panels that rotate on one-dimensional axial hinges. These models are not generalizable to thicker materials because when folded, the panels would interfere with each other. Much work has been done to overcome this challenge, and several thickness-accommodation techniques have been developed [1–7].

In addition to these thickness-accommodation techniques, surrogate hinges have been developed [8], which use principles of compliant mechanisms to reduce the stiffness of a section of material. This enables a designer to create a hinge-like feature with reduced stiffness similar to a paper crease. This stiffness reduction is done by changing the geometry with cuts, rather than introducing a new material, enabling mechanisms to be designed and produced monolithically [9] (manufactured from a single sheet).

## 1.2 New Avenues for Origami Design: Conceal-and-Reveal Mechanisms

Chapter 2 introduces a type of system called "conceal-and-reveal." As the field of thick origami is relatively new and expanding, there is an opportunity to find new types of systems that can be produced using origami techniques. This work defines conceal-and-reveal systems and shows how origami is a natural basis for their development. A conceal-and-reveal system is a device which has two states concealing and revealing a payload and undergoes continuous motion between these two states. Chapter 2 introduces and defines this type of system, presents a systematic method for designing it using thick, rigid materials, and demonstrates examples of designing devices using this process.

The process outlined in this chapter builds upon research done by Jessica Morgan [10] on design methods for origami mechanisms. It is generalizable to design any origami-adapted mechanism made from thick materials.

## 1.3 Origami Electronics: Regional Stiffness Reduction for Printed Circuit Board Design

Chapter 3 details an approach for using compliant mechanisms to reduce the regional stiffness of electronic printed circuit boards (PCBs) to produce rigid and flexible sections on the same PCB. Traditional PCBs are fabricated with copper-clad fiberglass. These are robust and inexpensive, but are rigid and incapable of producing the large deflections required in flexible electronics applications. Flexible electronics generally employ materials with low stiffness that enable large deflections [11]. However, material properties are global, and large deflections can induce stress on electronic components, which can lead to failure [12, 13]. The approach outlined here uses surrogate hinges to reduce stiffness in regions of the PCB substrate while leaving other regions rigid. This enables components to be placed in regions of rigidity to avoid high stresses induced by large material deflection. PCBs with flexible hinges can be fabricated from a monolithic sheet of rigid fiberglass using current standard manufacturing processes.

This technology enables PCBs to be used in origami design. It allows designs such as the origami flasher solar array [1] to be fabricated from a single sheet and contain working electrical circuits. Analytical and finite element models are developed and verified, and physical testing es-

tablish the robustness of the method. Prototypes are produced which demonstrate how this method could be used.

### 1.4 Computational Method for Optimization of Surrogate Hinges in Origami Design

Chapter 4 presents an approach for using computational optimization methods to design surrogate hinges using arrayed lamina emergent torsional (LET) joints [14]. Arrayed LET joints include many independent design variables, creating an under-constrained design problem. This slows design iteration and makes it difficult to find an optimal solution using trial-and-error. Optimization techniques are used to improve this process. Mixed integer techniques are employed to select design variables and produce a design which satisfies constraints and can minimize various objective functions such as stress and design footprint.

### 1.5 Research Objectives

The objective of this research is to develop and demonstrate new approaches for thick origami design. These methods add to the set of tools designers have to adapt origami principles to their design applications. Three major contributions are presented. First, the conceal-and-reveal class of systems is introduced. This expands the use case of origami mechanisms and facilitates origami-adapted design in new areas of application. Second, an approach is developed to design monolithic PCBs with regions of flexibility and rigidity. This enables novel origami and non-origami PCB designs. Third, an approach for optimizing surrogate hinges for origami design is presented. This speeds up the design of surrogate-hinge-based thick-origami mechanisms and automates the handling of design constraints and stress minimization.

# CHAPTER 2. ORIGAMI-BASED DESIGN OF CONCEAL-AND-REVEAL SYSTEMS

## 2.1 Introduction

This chapter presents "conceal-and-reveal" motion, wherein a payload is covered or protected (concealed) and is uncovered or exposed (revealed). The resulting mechanism provides continuous motion between the concealing state and revealing state.

Conceal-and-reveal motion is advantageous in a variety of engineering settings. For example, clandestine systems that require the payload (e.g. communication systems) to be shielded from detection until their use, are consistent with needs in some covert operations. Some scientific instruments (e.g. short-life sensors) need to be protected from harsh environments until a specified initiation event. High-end consumer products can benefit from packaging that presents the product (e.g. luxury cosmetics) in a way that validates value to the consumer. Many medical devices (e.g. sharp surgical instruments) are best contained until their use, but must be quickly and easily accessible when needed. Some devices are best protected during deployment (e.g. space systems during launch) and revealed when in their final position.

Origami is an ideal starting point for designing conceal-and-reveal motion because it has folded and unfolded states. In addition, origami mechanisms are made of multiple panels, which can cover and protect the payload in the mechanism's concealed state.

Engineers are increasingly looking to origami to create unique mechanisms and solve design problems. Recent years have brought advances in the understanding of the mathematical principles of origami as well as approaches to adapting these principles to the field of mechanical design. Origami solutions have been used for diverse applications such as reconfigurable mechanisms [15, 16], metamaterials [17], and DNA nanostructures [18]. Origami-based engineering design can provide an elegant approach to solving design problems, and systematic methods of synthesizing origami-adapted mechanisms can improve the process of solving these problems [19].

Many engineering applications require materials that are stiffer, stronger, thicker, and more rigid than paper. Adapting origami patterns to use these materials is non-trivial, and techniques have been developed to facilitate this adaptation [20].

Because most conceal-and-reveal applications require rigid materials with nonzero thickness (as opposed to near-zero-thickness paper origami), a design process for developing thick, rigid origami-adapted mechanisms for conceal-and-reveal motion is needed. The resulting method is general enough to apply to other applications with little modification, but is demonstrated here with three conceal-and-reveal examples.

## 2.2 Background

### 2.2.1 Origami in Engineering Design

Origami is an attractive inspiration for engineering design because it exhibits characteristics such as portability, stowability, and deployability [21]. Products designed using origami include deployable solar panel arrays [1], stowable optical apertures [22], highly compressible bellows [23], and automotive airbags [24]. Designs that incorporate both folded and unfolded states have been used in civil engineering and architecture [25]. As new techniques continue to be developed for transferring origami principles to engineering designs, it is anticipated that these applications will continue to expand.

### 2.2.2 Rigid Origami and Thick Origami

Mathematical and kinematic models have been developed to predict origami motion from a given fold pattern [26–29] and to design fold patterns based on a desired form [30–32]. When modeling origami, a zero-thickness assumption is used to approximate paper and other thin, sheet-like materials. However, this assumption does not hold when thicker materials are used. Rigid materials also present challenges in adapting origami patterns because hinges add complexity over paper creases.

Rigid-origami mechanisms and thick-origami mechanisms are subsets of origami-adapted mechanisms that present unique design challenges (see Fig. 2.1). It is important to address these challenges because many engineering applications require rigid, thick materials.

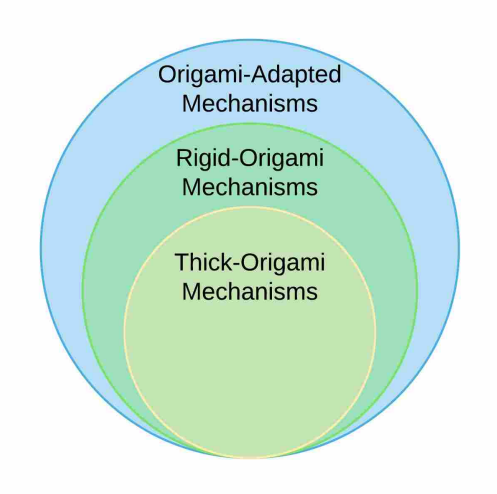


Figure 2.1: Thick-origami mechanisms and rigid-origami mechanisms are subsets of origami-adapted mechanisms.

When designing origami using rigid materials, an important property to consider is rigid foldability. Rigid-foldable origami patterns are patterns that can undergo a transformation from their unfolded to folded state with their panels remaining rigid and deformation occurring only at crease lines [33]. The rules for determining whether a given origami pattern is rigid foldable are well-understood [34–38], which helps designers evaluate fold patterns for potential suitability in rigid applications.

Several methods have been demonstrated for accommodating thick materials in origami-adapted engineering design. They include the Axis Shift method [2], the Offset Joint method [3,4], the Membrane Folds method [1], the Tapered Panels method [2], the Offset Crease method [5], the Spatial Linkages method [6], and the Offset Panel method [7]. These methods give designers a set of tools from which they can select a technique that is suitable for their design application. Morgan et al. [39] present a comparison of these thickness-accommodation techniques.

### 2.2.3 Design Process

Designing origami-adapted mechanisms can be a complex process with interrelated design decisions that are difficult to decompose [40]. To address this, Morgan et al. [41] proposed a preliminary design process for origami-adapted mechanisms similar to design processes for biomimetic design [42] and further developed this process for aerospace applications [43]. Four categories of material and design options used in origami-adapted design are outlined:

- Flexible Interrupted: flexible panels with cuts or slits
- Flexible Continuous: layers of flexible material
- Rigid Interrupted: rigid panels with cuts, slits, or pin hinges
- Rigid Continuous/Hybrid: rigid panels with a flexible membrane

The approach presented in this paper addresses Rigid Interrupted and Rigid Continuous/Hybrid origami-adapted designs. It may be used for thick, rigid origami in any application.

## 2.3 Conceal-and-Reveal Motion

This work presents a method to synthesize origami-based systems that undergo specified motion. We define a conceal-and-reveal system as one that is characterized by a starting state which conceals or protects a payload, an ending state which reveals or exposes the payload, and continuous motion between the two states.

Features of a conceal-and-reveal system as defined here include:

- The system has two terminal states: one in which the payload is concealed and one in which it is revealed
- The system undergoes continuous motion between these two states
- The payload is completely enclosed in the concealed state
- The payload is lifted out of its enclosure and presented in the revealed state

- The system has the number of degrees of freedom consistent with the needs of the application (often one degree of freedom)

Origami is well-suited to be the basis for these systems because origami has at least two states: folded and unfolded. Origami mechanisms are based on panel-shaped links which provide surfaces to cover the payload in the concealed state. The rules of rigid-foldability [44, 45] and thickness accommodation [2] are increasingly well-understood. Origami mechanisms are compact and have been used to pack designs in small volumes for stowing [46].

Because of the potential complexity of origami mechanisms, it is advantageous to use a systematic process in their design. The following section outlines a process for thick, rigid origami mechanisms intended for the design of conceal-and-reveal mechanisms but is general enough to apply to other systems.

## 2.4 Method

A six-step process for designing thick, rigid origami-adapted systems was developed in this work and is presented in Fig. 2.2. The steps of this process guide designers from low-fidelity concepts to increasingly high-fidelity designs.

### 2.4.1 Define Problem

The first step is to define the objective, design requirements, and constraints of the system. These are captured in a document such as a requirements matrix, which will guide the design later in the process. Methods for developing a requirements matrix can be found in design texts [47]. A requirements matrix provides constraints in design exploration and focuses designers on metrics that will lead to a successful design.

### 2.4.2 Select Origami Pattern

The next step is to select the origami pattern that will form the "seed" of the overall design. The designer explores the design space broadly. It is not necessary that the seed origami pattern exhibit the final desired motion of the mechanism. It is more important that the pattern have properties conducive to the material to be used, such as rigid foldability.

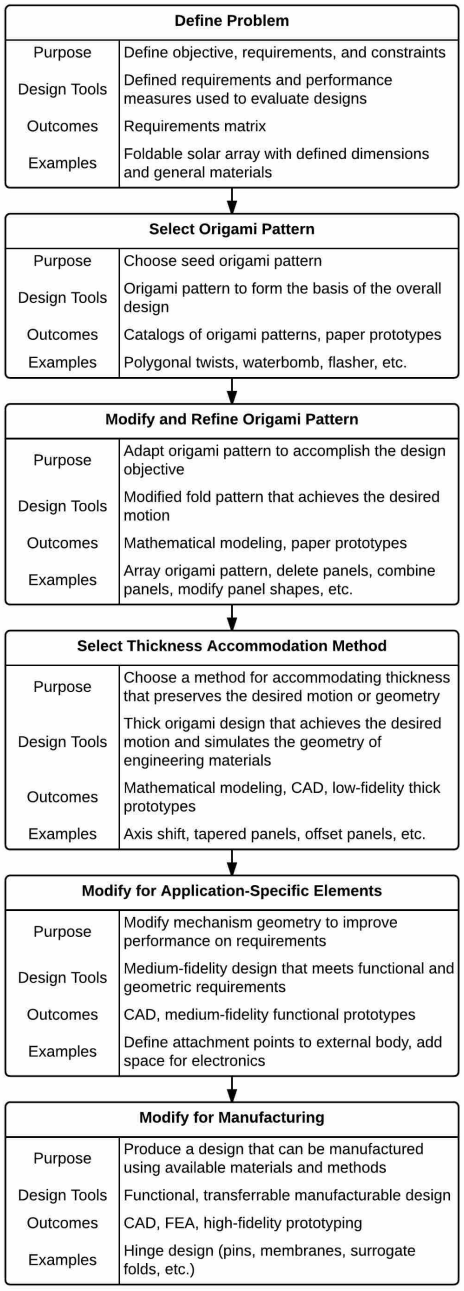


Figure 2.2: This chart introduces a process for designing thick, rigid-origami mechanisms. It is applied to produce origami mechanisms that exhibit conceal-and-reveal motion.

Unfortunately, a comprehensive library of origami patterns does not currently exist. However, there are resources which give partial sets of origami patterns [33] and describe varieties of origami principles [28, 48, 49].

### 2.4.3 Modify and Refine Origami Pattern

Once a seed origami pattern is chosen, it is modified and refined to achieve the desired motion. Three general types of origami pattern modification are:

- Tessellating the entire origami pattern or part of the pattern
- Adding or deleting panels
- Altering panel shape

These types of modification may also be combined, and computer-aided methods may be incorporated [50]. The result of this step is a pattern that exhibits the desired motion in a zero-thickness approximation (e.g. paper).

There is no set linear process to synthesize a crease pattern modification for a given situation. Rather, it is an iterative process that requires some intuition from the designer. Some guiding principles of this step include the following:

- The modified crease pattern should form a kinematic backbone compatible with the requirements outlined in Step 1.
- The modified crease pattern should preserve the desired number of degrees of freedom of the system.
- The modified crease pattern should not self-intersect when manufactured with thick materials and thickness-accommodation methods.

3-dimensional CAD models consisting of 2-dimensional panels with kinematic constraints can be useful in exploring the possible designs at this step in the process. Paper prototypes can also be helpful in visualizing candidate designs. As with the previous step, broad exploration of the design space is appropriate in this step. Since it is less difficult and more inexpensive to prototype in this stage than later ones, many possibilities can be explored, evaluated, and carried on to the next step.

### 2.4.4 Select Thickness-Accommodation Method

After the origami pattern is adapted to achieve the desired motion, it must be modified to accommodate thick, rigid materials. Several techniques have been developed to accomplish this goal [1–7]. Each is preferable under different circumstances, and their properties and tradeoffs should be considered. Morgan [39] has compiled a list of thickness-accommodation techniques and has compared their characteristics. This characterization is helpful in selecting a suitable means of accommodating thickness in the design. A thickness-accommodation method may be selected and modeled using mathematical methods and CAD software to verify its feasibility. In this step, designers can begin to fabricate thick prototypes and gain an understanding of how the mechanism will behave when made with engineering materials. Due to the increasing complexity and fidelity of the design during this phase, designers should narrow the set of candidate designs at this point.

### 2.4.5 Modify for Application-Specific Elements

At this point there will likely be application-specific aspects of the design that have not been addressed yet. When a suitable thickness-accommodation method has been selected, the overall design can be modified to address these design aspects. For example, the design may have to be altered to accommodate external parts or assemblies. In the case of conceal-and-reveal mechanisms, the payload must be accommodated.

As applications and design requirements vary, many approaches can be taken to modify the thick origami design. This can often be an iterative process that requires adjustment to the designs produced in the previous steps.

Mathematical and computer models are employed to design modifications to the crease patterns. These modifications could be changes to the pattern similar to those outlined in the previous step, or they could be additional structures added to the design and kinematically coupled.

During this step, it may become apparent that certain designs are less desirable than others, and as candidate designs are pruned, designers can focus on increasing the fidelity of the most promising designs. CAD models and medium-fidelity prototypes (such as with foam board, 3D-printed polymer, or wood) may be produced to aid in this step.

Once application-specific elements have been included in the design, a functional prototype can be produced and tested to verify that it meets the functional requirements of the design.

### 2.4.6 Modify for Manufacturing

Once a functional design has been made, the final materials can be selected and the manufacturing processes can be chosen. Materials and manufacturing processes depend mostly on the application requirements from the first step, with additional modifications which may be necessary to accommodate designs developed in the later stages of the process. In addition, origami-adapted systems can often be manufactured from a flat sheet or set of sheets, and this fact can be utilized in this step to simplify the manufacturing process. Once final materials and processes are chosen, a high-fidelity prototype can be constructed and tested to verify that it meets the design requirements.

## 2.5 Examples

The proposed process is demonstrated here through the design of three origami-based conceal-and-reveal mechanisms. Sharing an overall design objective among the three devices enables the discussion to focus on the process rather than the application. It also illustrates the ability to design multiple origami-based systems that satisfy a given design need.

The first step (Define Problem) is first presented and used for all three examples. Steps 2-6 were then performed for each example independently.

### 2.5.1 Problem Definition

The design objective is to create a conceal-and-reveal system that presents a luxury product to a consumer. The product used here is a high-end wrist watch. The conceal-and-reveal motion is important in expressing value to the consumer, who may be paying a lot for a product (in the case of high-end wrist watches, this can be hundreds of thousands of US dollars or hundreds of thousands of Euros) and there is an expectation that it is differentiated from its less-expensive counterparts. Several design requirements were identified through collaboration with an international luxury consumer product company:

- The mechanism should reveal the payload as the container is opened.

- The mechanism should lift the payload out of the container and present it to the user.
- The mechanism should provide additional concealment of the payload besides the lid of the container.
- The mechanism should combine rotational and translational movement of different parts of the mechanism.
- The conceal-and-reveal mechanism should fit inside a box-like container.
- The exterior of the container should resemble a standard watch box in the concealed state.
- The mechanism should utilize similar manufacturing methods as the rest of the container.

The next five steps in the design process are used to create three conceal-and-reveal devices with each based on a different origami seed pattern. The following sections describe how each pattern was adapted to form a unique solution to the problem.

## 2.6 Example 1: Square Twist Array

The first example design is the Square Twist Array. The resulting design uses an array of four Square Twist origami patterns with a flexible link that lifts the payload from the box.

### 2.6.1 Origami Pattern Selection

The square twist is a fundamental origami fold pattern shown in Fig. 2.3a. It is rigidly-foldable in certain configurations [38], which means the panels remain rigid throughout their motion, with all deflection occurring on the fold lines. This property makes it well-suited for applications that use thick, rigid materials [39]. The square twist pattern was selected as the basis for the first design example because of its simplicity and rigid-foldability.

### 2.6.2 Pattern Modification

To achieve conceal-and-reveal behavior, the square twist pattern was placed in a 2x2 array, as shown in Fig. 2.3b. Adjacent panels from each of the arrayed square twists were combined,

and the outside panels were removed. This left the 9 panels shown in Fig. 2.3c. The result was a mechanism with a single degree of freedom; the open and closed configurations are shown in Fig. 2.4.

As shown in Fig. 2.4, the outside panels close over the center of the pattern completely when the pattern is in its concealed state; thus, the payload will be completely covered. In its revealed state, the system opens the center panel and completely exposes it. This behavior shows promise for solving the conceal-and-reveal design problem outlined above.

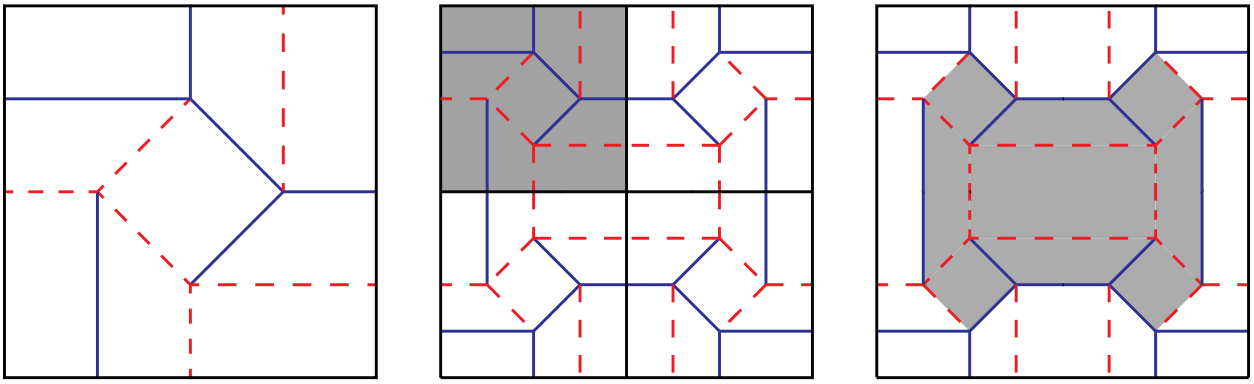

(a) (b) (c)

Figure 2.3: Square twist origami pattern modified for conceal-and-reveal behavior. (a) Original square twist fold pattern. Blue solid lines represent mountain folds, and red dashed lines represent valley folds. (b) Four arrayed square twists. This is the intermediate step to get from the square twist on the left to the modified pattern on the right. (c) Modified square twist pattern. The grey area indicates the portion used in this mechanism.

### 2.6.3 Thickness Accommodation

The Offset Panels Technique [7] was used for thickness accommodation. In the Offset Panels Technique, all hinges are placed on a single joint plane, and the panels are offset from that plane to accommodate for panel thickness when folded. Advantages of this technique include the preservation of pattern kinematics and range of motion, as well as the ability to maintain a single degree of freedom [39]. This enabled the pattern to be manufactured using thick materials while preserving the properties of the original origami pattern. Figure 2.5 shows a CAD model of the

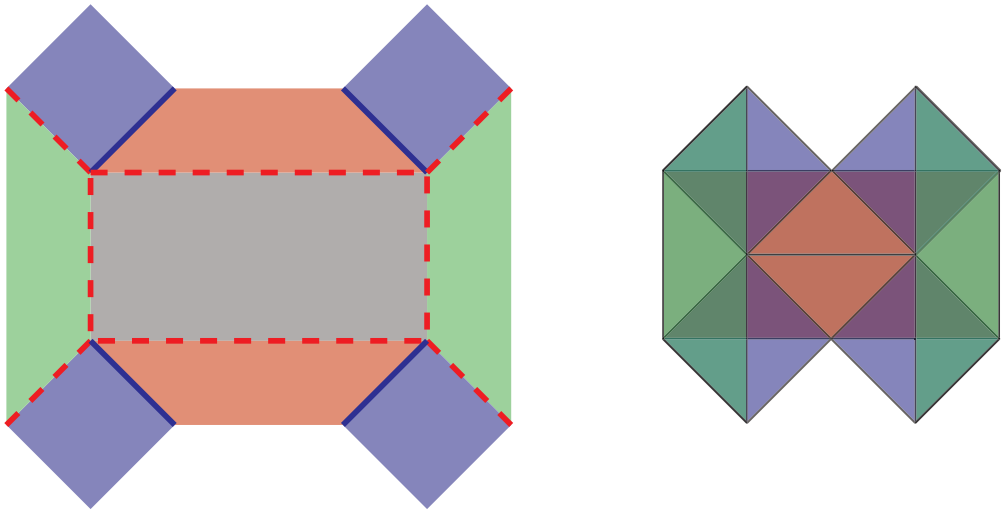

(a) (b)

Figure 2.4: An illustration of the revealed (left) and concealed (right) configurations of the arrayed square-twist pattern. Colors represent different layers in the closed configuration and correspond to the colors in Fig. 2.5.

resulting thick origami mechanism attached to an open box. The panels in Fig. 2.5 correspond to similarly-colored panels in Fig. 2.4.

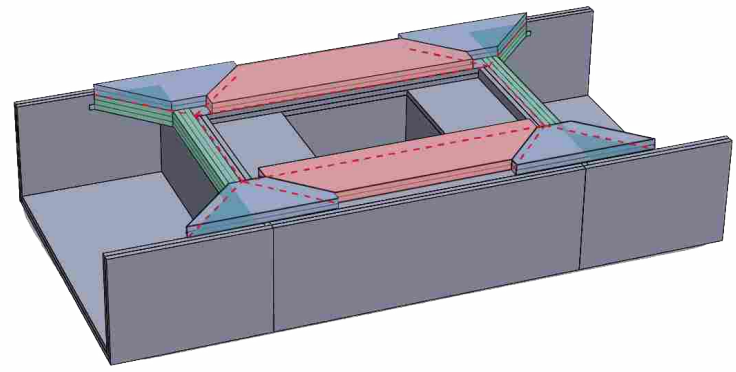

Figure 2.5: A CAD model of the Square Twist Array attached to an open box. The colors of the panels correspond to the colors in Fig. 2.4.

### 2.6.4 Payload Accommodation

A basic approach to accommodate the payload is to add a stationary compartment in the center panel for the payload. Although this would allow the payload to be concealed and revealed upon deployment, it would not provide the required lifting presentation. As shown in Fig. 2.5, a portion of the center panel was removed to accommodate the payload volume. A lift mechanism was designed to couple the motion of the panels with the payload. This preserves the single degree of freedom of the origami pattern. As the box is opened, the panel kinematics lift the payload in the same motion. Figure 2.6 shows a section view of the lift mechanism.

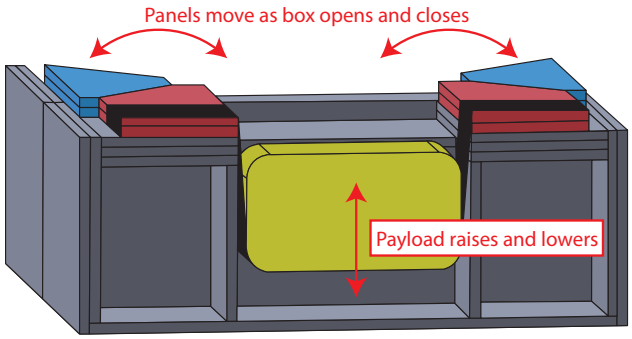


Figure 2.6: Section view of the payload and lift mechanism of the Square Twist Array. The yellow block represents the payload. When the panels open and close, the black strip translates their motion to lift the payload up and down.

### 2.6.5 Modification for Manufacturing

Once the design met the functional requirements of the conceal-and-reveal design problem, materials and manufacturing methods were addressed. Rigid boards were used as a core, covered by an adhesive paper membrane. This membrane served as a hinge between rigid sections. Figure 2.7 shows a prototype of the Square Twist Array conceal-and-reveal mechanism in two positions.

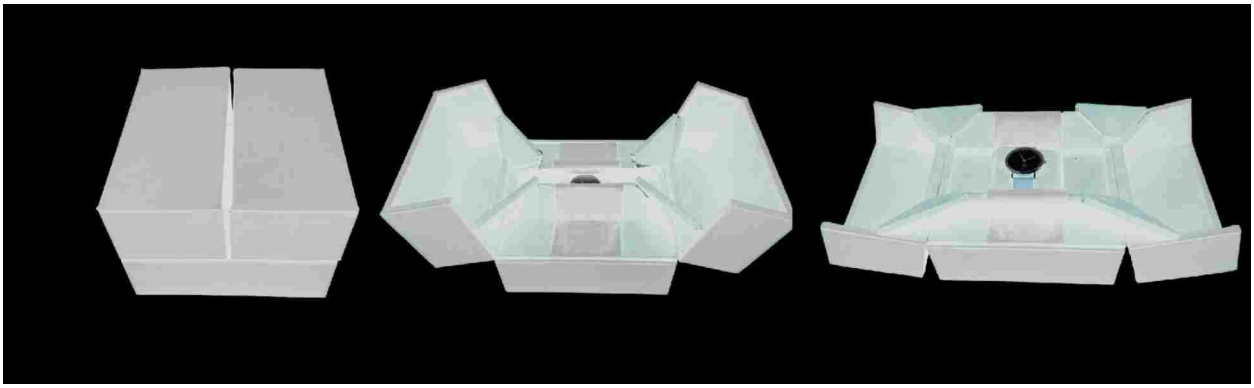

Figure 2.7: Prototype of Square Twist Array conceal-and-reveal mechanism.

## 2.7 Example 2: Modified Hexagon Twist

The second example design is the Modified Hexagon Twist. The resulting design employs the Hexagon Twist origami pattern and utilizes Sarrus linkages [51] to lift the payload from its stowed position inside the box.

### 2.7.1 Origami Pattern Selection

The Modified Hexagon Twist is based on rigidly foldable twists presented by Evans et al. [38]. The original pattern is shown in Fig. 2.8a. This pattern shares advantages with the Square Twist, such as rigid foldability, but does not need to be arrayed to conceal the payload.

### 2.7.2 Pattern Modification

The Hexagon Twist pattern was modified as shown in Fig. 2.8 to achieve conceal-and-reveal motion. The original origami pattern begins with a square outline, but the folded shape would not completely conceal the center panel. The outline of the pattern was therefor modified as shown in Fig. 2.8b.

### 2.7.3 Thickness Accommodation

The design was further modified to accommodate panel thickness. The Axis Shift thickness-accommodation method was selected because it required fewer offsets as compared to other thickness-

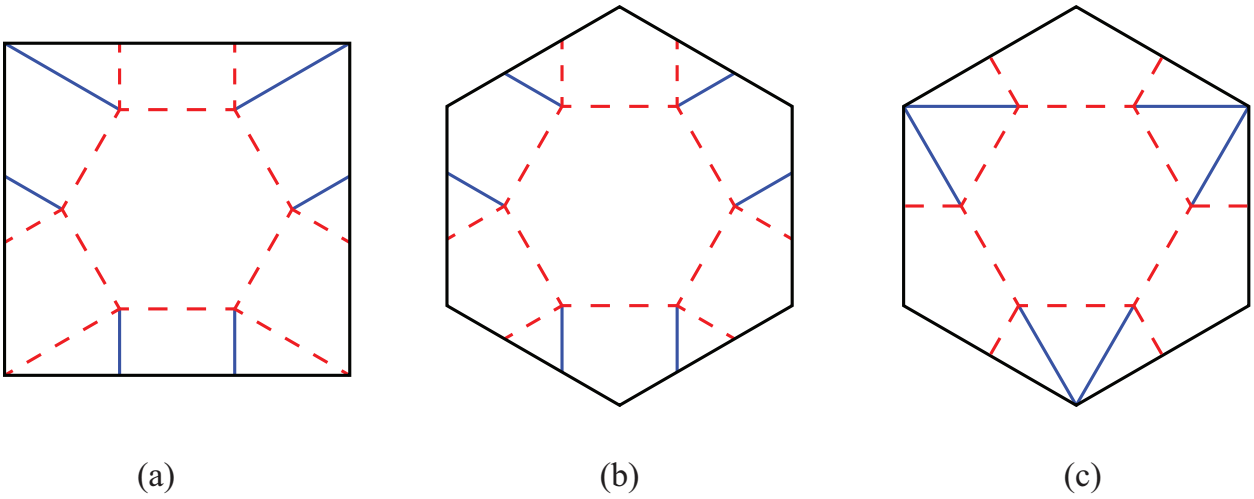

(a) (b) (c)

Figure 2.8: Modification of the hexagonal twist pattern. (a) Original hexagon twist pattern. Blue solid lines represent mountain folds, and red dashed lines represent valley folds. (b) Modification of exterior panels for conceal and reveal motion. (c) Modification of pattern for thickness accommodation using Axis Shift technique.

accommodation methods [2]. Its use of overconstrained spatial linkages also helps provide a rigid mechanism [6] that preserves one overall degree of freedom in the system. To accommodate this method, the pattern was adapted as shown in Fig. 2.8c. A functional prototype with thick panels is shown in Fig. 2.9.

### 2.7.4 Payload Accommodation

To achieve lifting presentation, a vertically translating compartment was added to the mechanism. Figure 2.10 shows the mechanism which lifts this compartment and the linkage which connects the panels to the lid to drive this motion. The compartment is an open triangular prism, and the lifting is achieved using a Sarrus linkage attached to the triangular panels of the Hexagon Twist (see Fig.2.11). The links of the Sarrus linkage undergo a 90° rotation from the fully extended configuration to the fully collapsed configuration. This limits the range of motion of the triangular panels, which are directly connected to the linkage. Because the triangular panels undergo less rotation than the larger panels when the pattern is first unfolding, the mechanism is able to completely reveal the payload as the larger panels unfold greater than 90°.

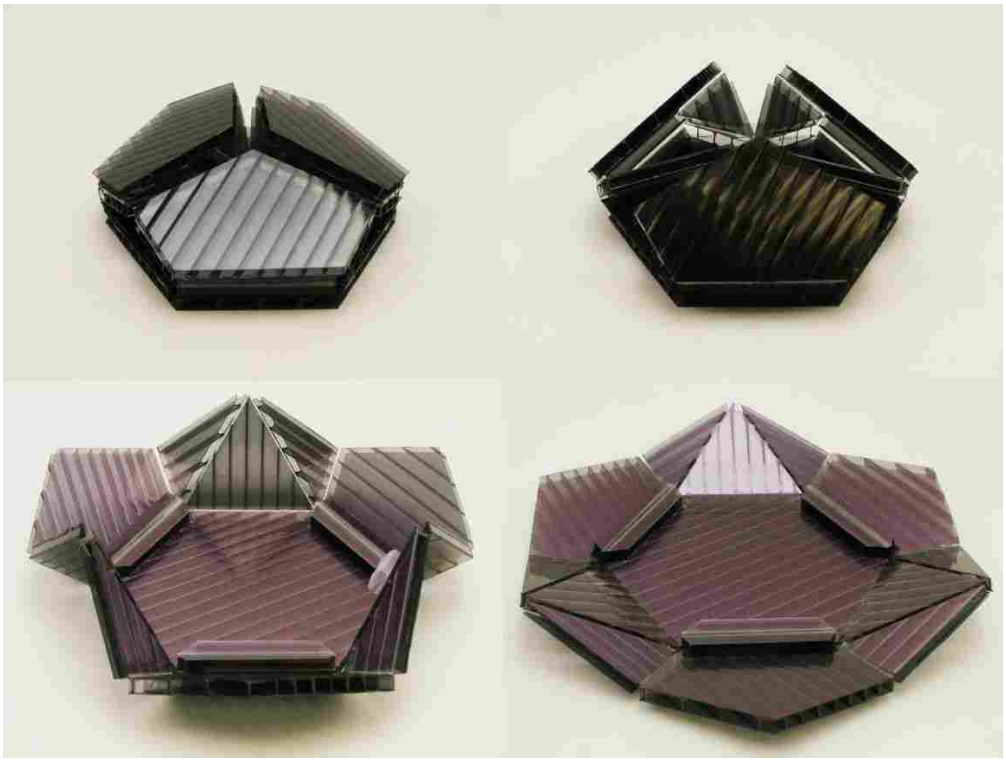

Figure 2.9: Modified Hexagon Twist with thick panels going through its folding motion.

### 2.7.5 Modification for Manufacturing

The origami mechanism and lifting apparatus were designed to be fabricated separately from the rest of the box and lid, as shown in Fig. 2.10. The whole system was then integrated and assembled as shown in Fig. 2.11. The motion of the mechanism is coupled to the lid using a four-bar linkage that is formed by the box base, the box lid, the large exterior panel of the hexagon twist, and a connecting link which connects the hexagonal exterior panel to the box lid (see Fig. 2.12). The length and position of this link relative to the box lid and Hexagon Twist exterior panel determine the relationship of the motion of the box's opening to the kinematics of the conceal-and-reveal motion. The length and position of this link were designed so that when the box lid opens 90°, the conceal-and-reveal mechanism is fully actuated.

This four-bar mechanism couples the opening of the lid to the opening of the origami mechanism, thus preserving the single degree of freedom motion. As the lid is opened, this four-bar linkage drives the origami pattern to open, which drives the motion of the Sarrus linkage to lift the payload compartment.

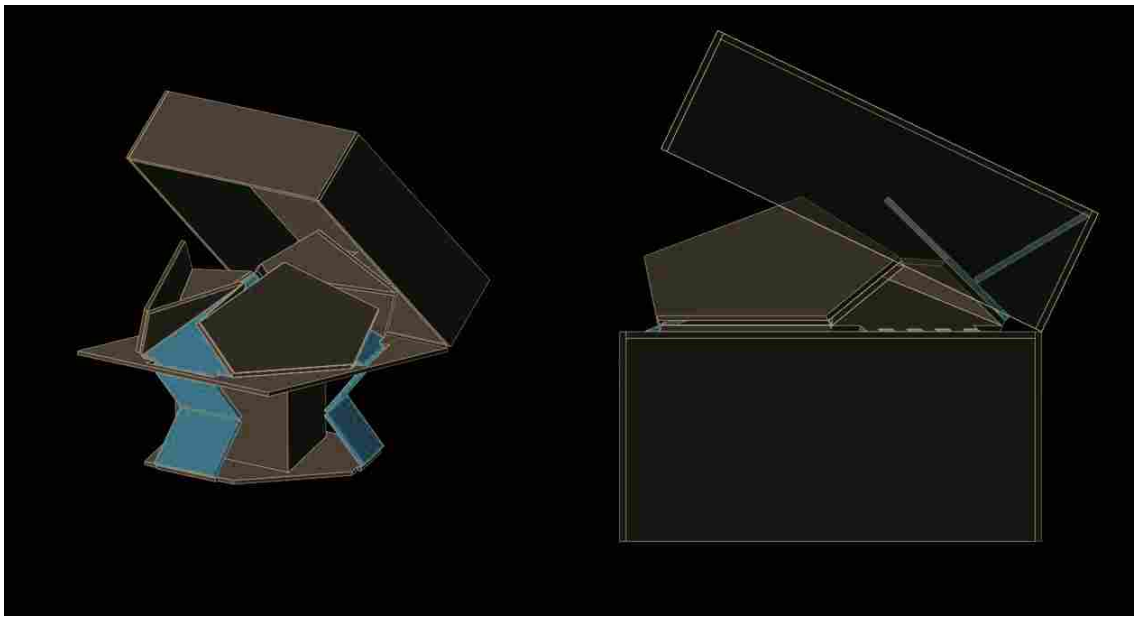

(a) (b)

Figure 2.10: Linkages for actuation. (a) Sarrus linkages (red) lift the payload as the panels open. (b) Links behind mechanism panels couple the motion of the panels with the motion of the lid.

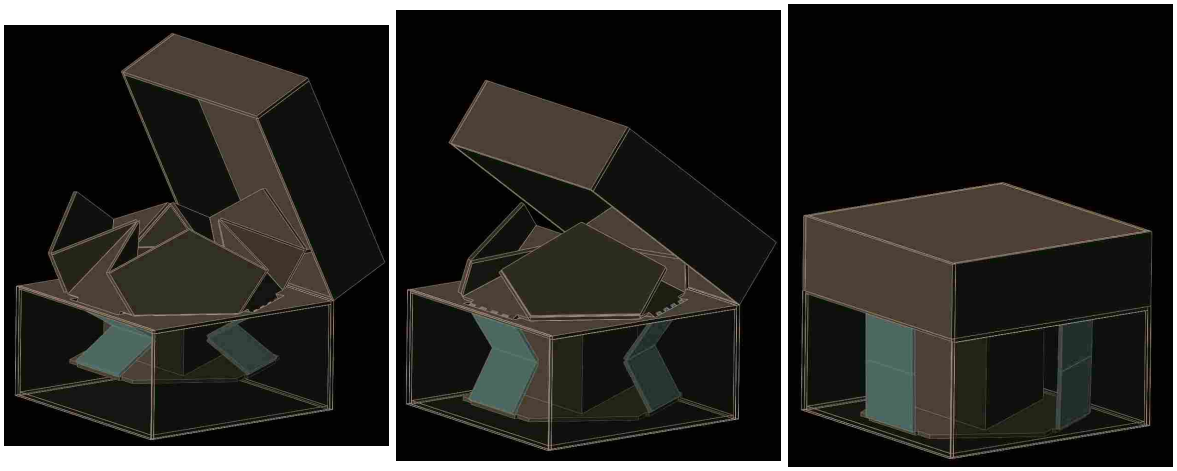

(a) (b) (c)

Figure 2.11: Sarrus mechanism (red) used in the actuation of the Modified Hexagon Array.

To assist the actuation of the mechanism, a compression spring was placed between the bottom of the box and the bottom of the Sarrus mechanism (see Fig. 2.13). This makes the opening and closing of the box bistable. When the box is in the conceal state, the links of the Sarrus mechanism are fully extended and the mechanical advantage of the bottom of the Sarrus mechanism

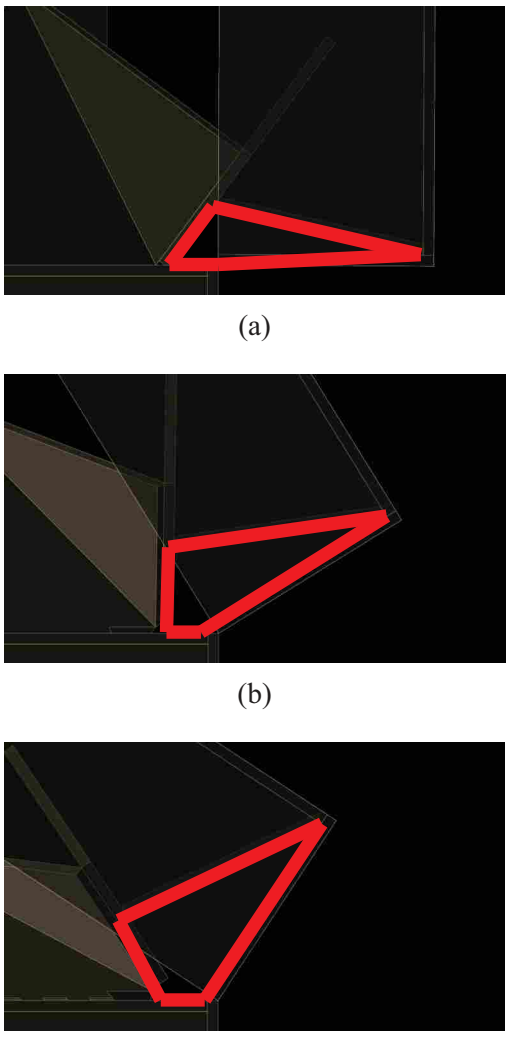

(a)

(b)

(c)

Figure 2.12: Four-bar mechanism (red) formed by links coupling the motion of the origami array with the lid. Images show mechanism starting (a) fully open and (b,c) going through closing motion.

in relation to the movement of the lid is low. Because of this, the spring alone is unable to open the box. When the box is in the reveal state, the Sarrus linkage is collapsed and the spring is able to keep the box open because of the higher mechanical advantage of the Sarrus linkage in this position.

Figure 2.14 shows a prototype of the Modified Hexagon Twist conceal-and-reveal mechanism in its concealed, intermediate, and revealed positions.

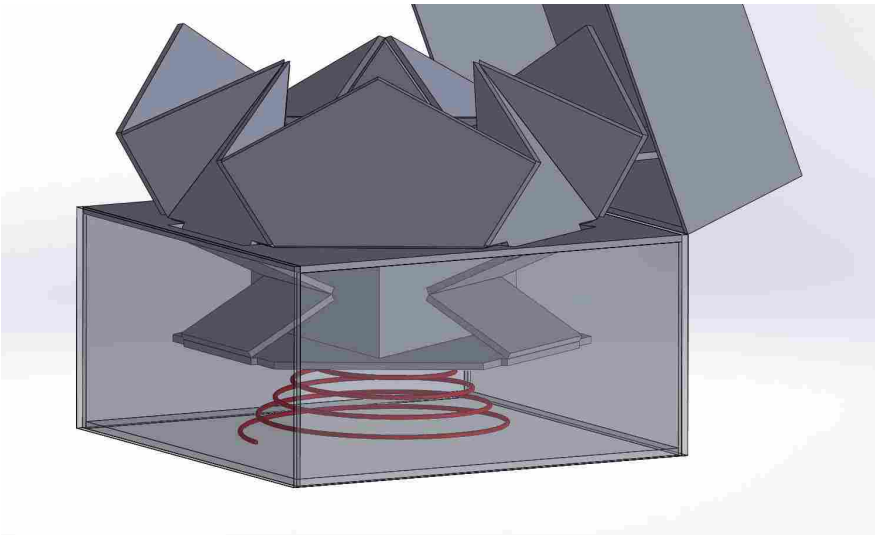

Figure 2.13: A compression spring (red) assists with the actuation of the Modified Hexagon Array.

Figure 2.14: Prototype of Modified Hexagon Twist conceal-and-reveal mechanism.

## 2.8 Example 3: Chicken Wire Tessellation

The third example design is the Chicken Wire Tessellation (also known as the Hexagonal Pattern). The resulting design takes advantage of the natural folding characteristics of the Chicken

Wire Tessellation pattern, requiring less modification from the original origami than the previous two designs.

### 2.8.1 Origami Pattern Selection

The Chicken Wire Tessellation is an origami pattern that consists of tessellated hexagons folded in half to form two trapezoids each (see Fig. 2.15). This pattern is related to the Yoshimura pattern [52] and is rigidly foldable [33]. As shown by Miura [53], it folds into a pseudo-cylindrical concave shell (see Fig. 2.16).

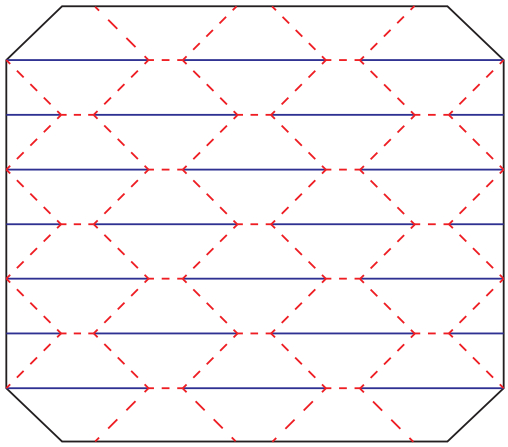

Figure 2.15: Chicken Wire Tessellation origami pattern. Blue solid lines represent mountain folds, and red dashed lines represent valley folds.

### 2.8.2 Pattern Modification

When folded, the Chicken Wire Tessellation self-intersects before folding flat (see Fig. 2.16). To avoid self-intersection, panels were modified as shown in Fig. 2.17. In the figure, panels marked with X's are deleted, and panels shaded gray are added. This enables the panels to fold flat in the concealed position and provides additional concealment.

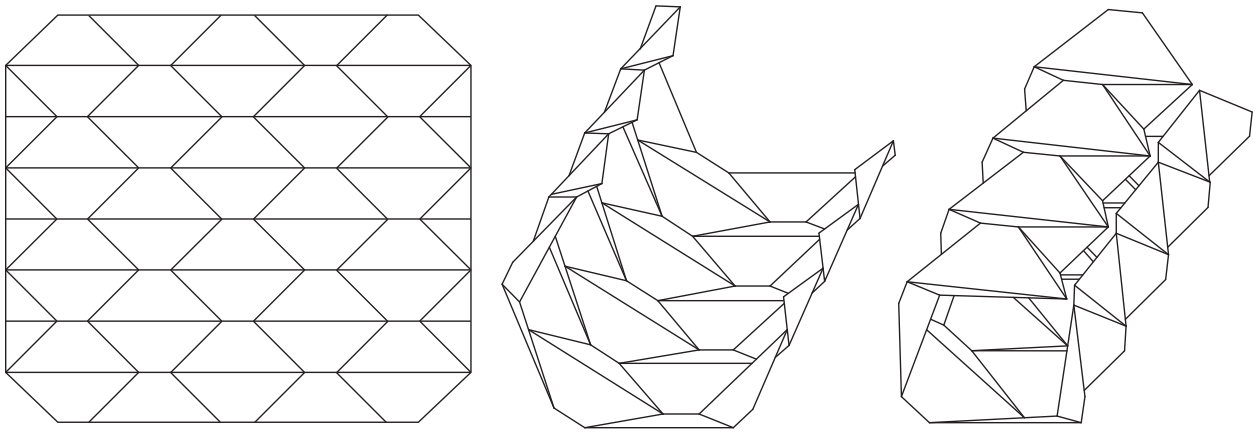

Figure 2.16: Chicken Wire Tessellation folding into a pseudo-cylindrical concave shell. Note that further motion is prevented by self-intersection. The pattern is modified to avoid this, as shown in Fig. 2.17.

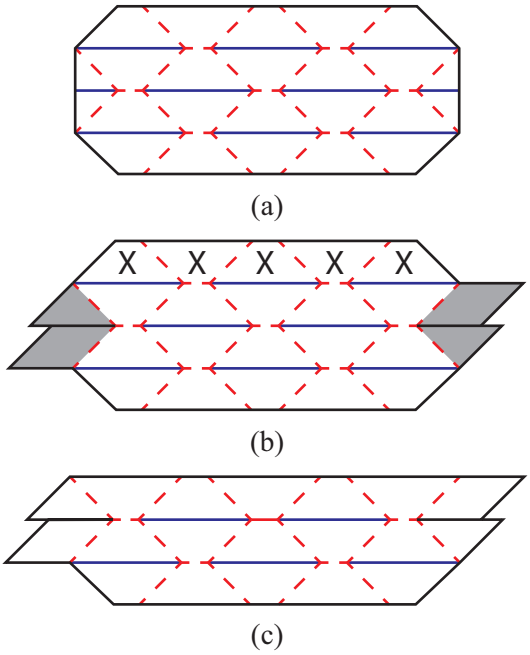


Figure 2.17: Modification of the Chicken Wire Tessellation Pattern. Panels labeled with X's are removed, and gray panels are added.

### 2.8.3 Thickness Accommodation

The Axis Shift thickness-accommodation method [2] was chosen for this design because it did not require the use of offsets for this pattern. The kinematics and range of motion of the

folding pattern were preserved. Thin membranes were used for hinges [1], and the pattern did not require any additional modification to accommodate thickness.

### 2.8.4 Payload Accommodation

A storage compartment was included in the base of the box to accommodate the payload when the box was closed, and a parallelogram linkage [54] was used to lift the payload out of the storage compartment when the box was opened (see Fig. 2.18). The parallelogram linkage was the width of the smallest edge of the tessellation, so it did not interfere with the origami pattern in any configuration. The linkage was attached to the origami mechanism so that their motion was coupled and combined, they have a single degree of freedom.

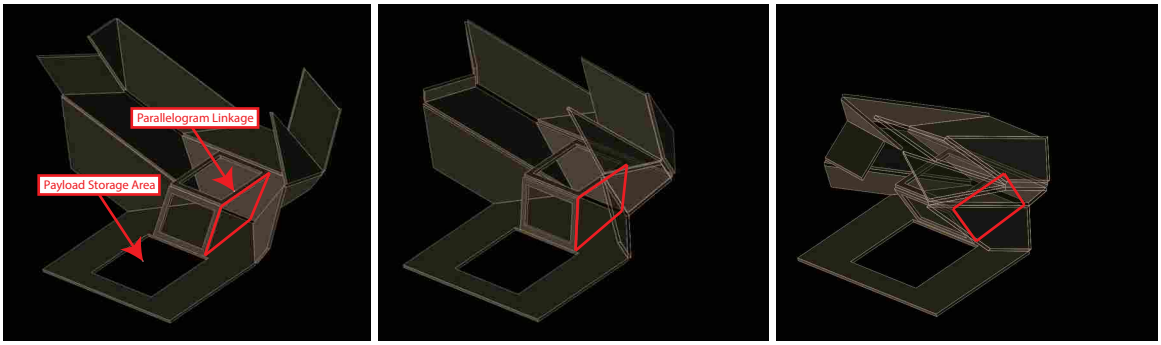


(a) (b) (c)

Figure 2.18: Parallelogram linkage (red) used to lift the payload out of storage for the Chicken Wire Tessellation conceal-and-reveal box.

### 2.8.5 Modification for Manufacturing

To integrate the Chicken Wire Tessellation into the outside box structure, panels from the top and bottom of the origami pattern were attached to the box lid and base. The parallel guiding mechanism was attached to origami panels and to the box base. This design allowed the origami portion of the design to be manufactured separately from the box and integrated in assembly. Figure 2.14 shows a prototype of the Chicken Wire Tessellation conceal-and-reveal mechanism in its concealed, intermediate, and revealed positions.

Figure 2.19: A prototype of the Chicken Wire Tessellation conceal-and-reveal mechanism.

## 2.9 Conclusion

This work introduces the "conceal-and-reveal" term to represent a type of system function that is useful in multiple engineering settings; presents the case for using origami-based designs to achieve the desired conceal-and-reveal behavior; proposes a six-step process for the design of thick, rigid origami-based systems; and demonstrates the process through the design and prototyping of three systems that share an overall design objective but employ different origami patterns and thickness accommodation techniques to achieve the objective.

Conceal-and-reveal systems use mechanisms to alternately cover and expose a payload. Origami is well-suited for designing these systems, and the design space is broad and largely unexplored. The method presented here is general enough to apply to a wide range of applications. It was demonstrated here with three solutions to one problem definition to clearly demonstrate the use of the method. The approach can be followed to address a variety of other conceal-and-reveal problems, including applications in medical devices, space systems, and covert operations, to name a few. The examples also demonstrated that a range of ridiidly-foldable origami patterns can be adapted for use in conceal-and-reveal mechanisms.

The design process introduced and demonstrated here can also be generalized to thick, rigid origami beyond conceal-and-reveal applications. It can be used in a variety of design applications

that utilize materials that are thicker and stiffer than paper. Other application-specific elements could be substituted, such as maximizing deployed surface area or minimizing volume required when stowing the mechanism. This design process gives designers a framework with which they may approach any design utilizing thick, rigid origami, and it may be adapted to meet the requirements of a specific situation.

# CHAPTER 3. REGIONAL STIFFNESS REDUCTION USING LAMINA EMERGENT TORSIONAL JOINTS FOR FLEXIBLE PRINTED CIRCUIT BOARD DESIGN

## 3.1 Introduction

Recent years have seen significant advances in flexible printed circuit board (PCB) technology. Flexible electronics are used in a wide array of industries, including aerospace, automotive, consumer electronics, and medical devices [11]. Increasingly demanding design requirements include flexibility, manufacturability, and fatigue life. These requirements often compete and lead to design trade-offs.

Flexible electronics research and development generally focus on developing and applying materials with low stiffness. Material properties are global and affect the entire PCB, so these trade-offs can cause undesirable behavior in some parts of the device. In particular, fatigue due to repeated deflection of components and their connecting joints can lead to failure [55]. It is desirable to limit the strain on components and connecting joints to increase the service life of the device.

In addition to material selection, increased flexibility can also be achieved using geometry and boundary conditions [56]. Compliant mechanisms are devices that achieve their motion from deflection of flexible components, and they have been used in electrical connectors to improve performance and reliability [57]. They have also been used to protect components from stresses due to impact [58].

This chapter presents an approach for reducing stiffness regionally using principles of compliant mechanisms to design for flexibility based on geometry. Surrogate hinges composed of arrayed lamina emergent torsional (LET) joints are used to introduce regions of flexibility while keeping areas of rigidity in a PCB made with a stiff substrate. The approach enables electronic components to be attached to rigid sections of the PCB while facilitating flexibility elsewhere.

## 3.2 Background

Various technologies exist for the design of flexible PCBs. These technologies provide inherent trade-offs compared to traditional rigid PCBs, which are often made with a copper conductive layer on a flame retardant fiberglass substrate.

### 3.2.1 Flexible Electronics

Similar to traditional rigid PCBs, flexible printed circuits include an electrically conductive coating adhered to an insulating substrate [11]. A wide variety of flexible conductors have been used and proposed, including metallic films [59], eutectic indium/gallium [60], percolated networks of conducting nanowires [61], polymers [62], and graphene [63]. Flexible substrates such as plastic films [64], metal foils [65], and textiles [66] have also been used and proposed. Using flexible materials results in a global reduction in stiffness, which leads to trade-offs in other properties (such as electrical conductivity or manufacturability).

The two main failure modes for flexible electronic devices are crack propagation and delamination [67, 68]. Failures are generally more common in the conductive layer than the substrate because the conductive layer must be optimized for things other than just mechanical strain (such as electrical conductivity) and it is farther away from the neutral bending axis [69]. In addition, components mounted in a flexible circuit experience strain at the mounting surface, either in compression (on the inside of the bend) or tension (outside of the bend), which can cause failure in the components [12, 13]. Fig. 3.1 illustrates the stress that is applied when flexible circuit boards are deflected. The effects of fatigue and high stress on electronic components have been studied [70, 71], and it is beneficial to reduce the fatigue and stress applied to these components.

Current solutions to this problem include adding stiffeners to flexible circuit boards and producing multi-layer printed circuit boards that include layers of flexible and rigid materials that are cut to allow for regions of flexibility and rigidity. Both of these approaches add cost and manufacturing complexity. They are also difficult to scale to the micro scale. Designing geometry that can add flexibility in specific regions while keeping others rigid could prevent high stresses from damaging components.

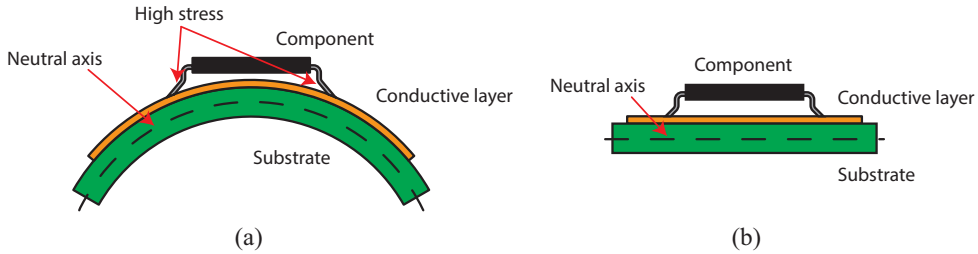


Figure 3.1: Current techniques for producing flexible electronics allow for uncontrolled deflection of the entire substrate. When the circuit is (a) undeflected, components and solder joints experience low stresses. When the circuit is (b) deflected, components and solder joints experience high stresses.

### 3.2.2 Surrogate Hinges

Flexible PCBs are fabricated in a plane and can exhibit motion out of their fabrication plane, and they can be categorized as lamina emergent mechanisms (LEMs). The field of compliant mechanism provides approaches for designing robust LEMs that can be fabricated on a planar sheet [72]. Surrogate hinges (also known as surrogate folds) are a class of mechanism that use compliant members to achieve a hinge-like motion. Various geometries for surrogate hinges have been developed [8] and evaluated for different loading conditions [9]. The Lamina Emergent Torsional (LET) joint [14] is one such geometry that transforms an overall deflection in bending to torsional deflection in its legs (See Figure 3.2a).

LET joints can also be arrayed in series and parallel (see Fig. 3.2b). This allows designers to use several LET joints to further reduce the stiffness.

## 3.3 Approach

To investigate the approach of using arrayed LET joints to reduce stiffness in printed circuit boards, the stresses were modeled analytically and using finite element analysis (FEA). These models were compared, and a prototype was constructed and tested.

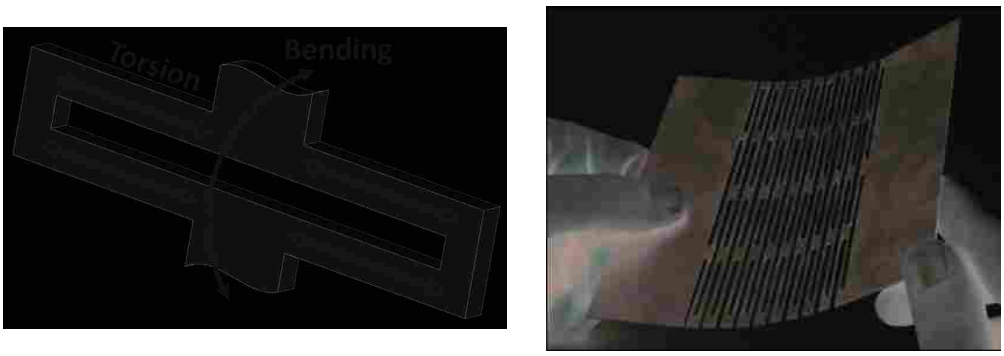


(a) (b)

Figure 3.2: (a) A single LET joint and (b) an array of LET joints. LET joint geometry lowers stiffness by transferring an applied bending load over the joint to torsional loads in the legs.

### 3.3.1 Models and Analysis

Analytical and FEA models were developed and compared to aid engineers in developing suitable geometry to implement these joints in a design application. The following sections describe these models.

#### Analytical Model

An analytical model was developed based on work done by Jacobsen et al. [14], where a single LET joint is analyzed (see Fig. 3.3). Figure 3.3b shows the parameters referenced in the equations below.

An applied pure moment is assumed, and the moment-deflection behavior is characterized by

$$M = k_{eq}\theta \tag{3.1}$$

where $M$ is the moment on the joint from the applied angular deflection $\theta$, and $k_{eq}$ is an equivalent spring constant based on a combination of the individual pseudo spring constants in the joint ($k_{1-6}$ in Fig. 3.3a). Figure 3.4 shows the applied angular deflection $\theta$ that induces moment $M$.

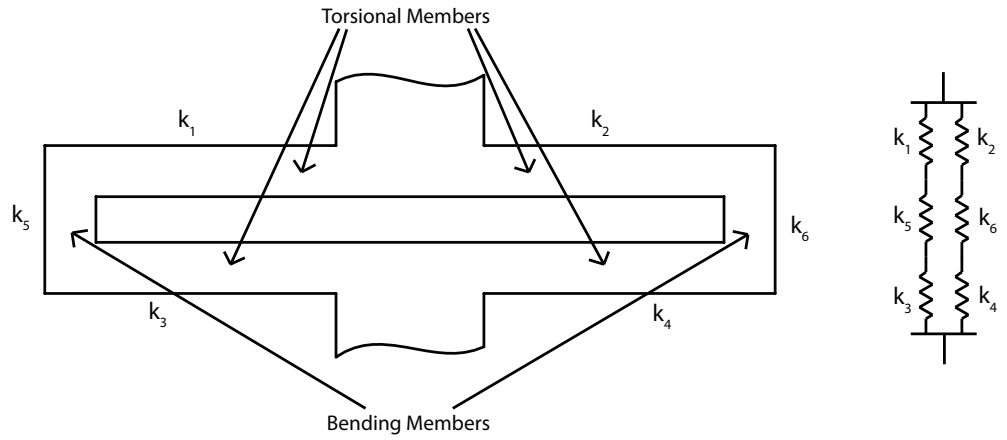


(a)

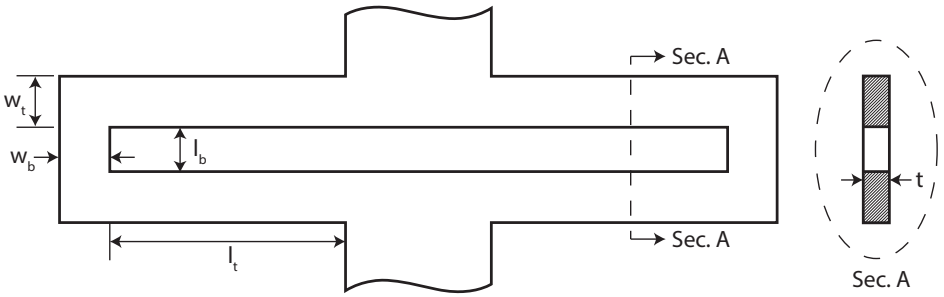


(b)

Figure 3.3: (a) A single LET joint with its corresponding spring system and (b) geometric parameters for Eq. 3.1-3.12.

Combining the springs from Figure 3.3a results in an equivalent spring constant of

$$k_{eq} = \frac{k_1 k_3 k_5}{k_1 k_3 + k_1 k_5 + k_3 k_5} + \frac{k_2 k_4 k_6}{k_2 k_4 + k_2 k_6 + k_4 k_6} \tag{3.2}$$

Assuming that a symmetric LET joint is used, $k_1 = k_2 = k_3 = k_4$ and $k_5 = k_6$. Since stiffnesses $k_{1-4}$ are the stiffnesses of the torsional members, they can be represented as $k_t$. Likewise, $k_{5-6}$ can be represented as $k_b$ for the stiffness of the bending members. Combining the above stiffnesses as springs in parallel and series (see Fig. 3.3a) yields the equivalent stiffness of a single LET joint in terms of the stiffness of its torsional and bending members:

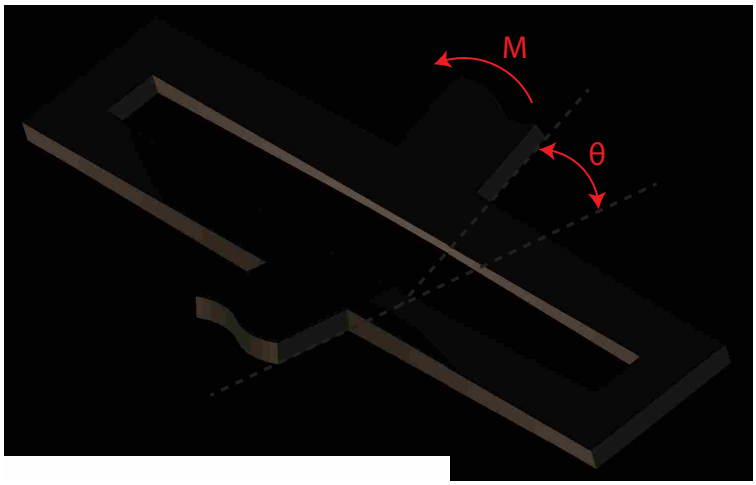


Figure 3.4: Deflected LET joint with parameters from Eq. 3.1 labeled.

$$k_{eq} = \frac{2k_t k_b}{k_t + 2k_b} \tag{3.3}$$

To find the total equivalent stiffness, the stiffnesses of the torsional and bending members is calculated. The torsional stiffness $k_t$ is calculated by

$$k_t = \frac{K_i G}{l_t} \tag{3.4}$$

where $G$ is the modulus of rigidity and $l_t$ is the length of the torsional segment. $K_i$ is a geometry-dependent parameter defined by

$$K_i = w_t t^3 \left[\frac{1}{3} - 0.21\frac{t}{w_t}\left(1 - \frac{t^4}{12w_t^4}\right)\right] \tag{3.5}$$

where $t$ is the thickness of the LET joint and $w_t$ is the width of the torsional segment.

The bending stiffness $k_b$ is calculated by

$$k_b = \frac{E w_b t^3}{12 l_b} \tag{3.6}$$

where $E$ is the modulus of elasticity, $w_b$ is the width of the bending member, and $l_b$ is the length of the bending member.

The shear stress in a non-circular torsion member can be modeled by the equation

$$\tau_{max} = \frac{T_i}{Q} \tag{3.7}$$

where $T_i$ is the torque applied to the torsional member and $Q$ is a geometry-dependent parameter, defined for a rectangular cross section as follows:

$$Q = \frac{w_t^2 t^2}{3w_t + 1.8t} \tag{3.8}$$

The bending stress in the bending members can be calculated by

$$\sigma_{max} = \frac{6T_i}{w_b t^2} \tag{3.9}$$

where $T_i$ is the torque applied to the bending member, $w_b$ is the width of the bending member, and $t$ is the thickness of the bending member.

It is important to note that $T_i$ for both shear and bending is equivalent to half of the moment applied to the joint, since there are two torsion and bending members in parallel and the load is shared. Therefore, $T_i$ is given as

$$T_i = \frac{M}{2} \tag{3.10}$$

for a single LET joint.

The maximum Von Mises stress, $\sigma_{max,v}$, can then be calculated from $\tau_{max}$ and $\sigma_{max}$ as

$$\sigma_{max,v} = \sqrt{\sigma_{max}^2 + 3\tau_{max}^2} \tag{3.11}$$

Combining equations 3.1 through 3.11, it is possible to determine the maximum stress in the joint with respect to the applied angular deflection $\theta$ as

$$\sigma_{max,v} = \frac{K_i G}{l_i}\theta\sqrt{\frac{9}{{w_b}^2 t^4} + \frac{3}{4Q^2}} \tag{3.12}$$

In cases where $m$ joints are arrayed in parallel, the torque on each joint is equal to the applied torque divided by $m$. In cases where $n$ joints are arrayed in series, the angular deflection

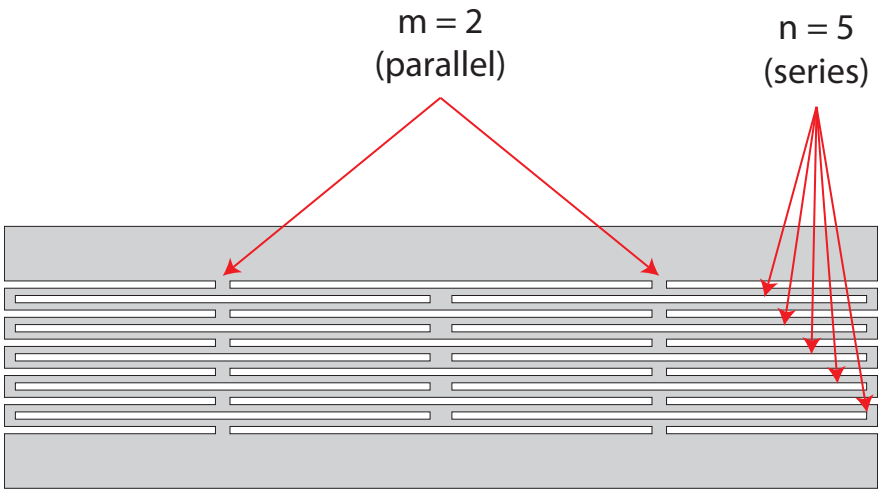


Figure 3.5: Detail view of LET joint array.

on each joint is equal to the total angular deflection divided by $n$. The maximum Von Mises stress of a LET joint array with $m$ joints in parallel and $n$ joints in series (see Fig. 3.5) is then given by

$$\sigma_{max,v} = \frac{2k_t k_b \theta}{n(k_t + 2k_b)} \sqrt{\frac{9}{w_b^2 t^4} + \frac{3}{4Q^2}} \tag{3.13}$$

Substituting Eqs. 3.4 and 3.6 into Eq. 13 yields

$$\sigma_{max,v} = \frac{2(\frac{K_i G}{l_t})(\frac{E w_b t^3}{12 l_b})}{(\frac{K_i G}{l_t}) + 2(\frac{E w_b t^3}{12 l_b})} \sqrt{\frac{9}{w_b^2 t^4} + \frac{3}{4Q^2}} \tag{3.14}$$

The above analytical model was verified using finite element analysis.

**FEA Model**

To verify the analytical model of the LET joint array in FEA, various $m$ x $n$ arrays of LET joints (with $m$ being the number of LET joints in parallel and $n$ being the number of LET joints in series) were modeled and then deflected to an angular displacement of 180°. ANSYS Parametric Design Language was used to perform the analysis. Solid186 elements were used to model the torsional members, and Beam188 elements were used to model the rigid regions at the ends of the design. The model was meshed into about 188 elements per torsional member. Because of the large deflection of the structure, a nonlinear solver was used.

The maximum Von Mises stress from the FEA solution was compared to the maximum Von Mises stress from the analytical model in Section 3.3.1. The comparison of the two models is presented in Table 3.1, along with the difference expressed as a percentage of the total Von Mises stress. Note that in all cases, the difference was within 8%. Sources of error include the assumptions that members were loaded in pure tension and bending and that all other components were rigid. In addition, stress concentrations led to higher maximum stresses in the FEA model. A stress concentration factor of 1.07 accounts for the difference beween the analytical and finite element models.

Table 3.1: Comparison of analytical and finite element model results. The Von Mises stress is listed, based on a 180° angular displacement load. Note that $m$ is the number of LET joints in parallel and $n$ is the number of LET joints in series (see Fig. 3.5).

| Array Size ($m$x$n$) | Analytical Max Stress (MPa) | FEA Max Stress (MPa) | Error (%) |
|---|---|---|---|
| 1x1 | 1658.5 | 1746.0 | 5.28 |
| 1x2 | 829.3 | 887.4 | 7.01 |
| 1x3 | 552.8 | 593.6 | 7.38 |
| 1x4 | 414.6 | 445.3 | 7.40 |
| 1x5 | 331.7 | 357.0 | 7.63 |
| 1x6 | 276.4 | 297.4 | 7.61 |
| 1x7 | 236.9 | 255.2 | 7.72 |
| 2x1 | 1658.5 | 1757.3 | 7.82 |
| 2x2 | 829.3 | 887.0 | 6.96 |
| 2x8 | 207.3 | 223.7 | 7.91 |
| 2x10 | 165.9 | 178.8 | 7.82 |

### 3.3.2 Prototype Design

The validated models in Section 3.3.1 facilitate the design of electronic devices with regions of flexibility and rigidity. One such design was prototyped and tested to investigate the feasibility of using arrayed LET joints as a means of introducing flexibility in rigid printed circuit boards.

Figure 3.6 shows the device that was constructed to demonstrate this concept in practice. The prototype is a folding solar array with the solar panels electrically connected in series with traces in the LET joints. The device is designed to fold 180° and stow in a backpack.

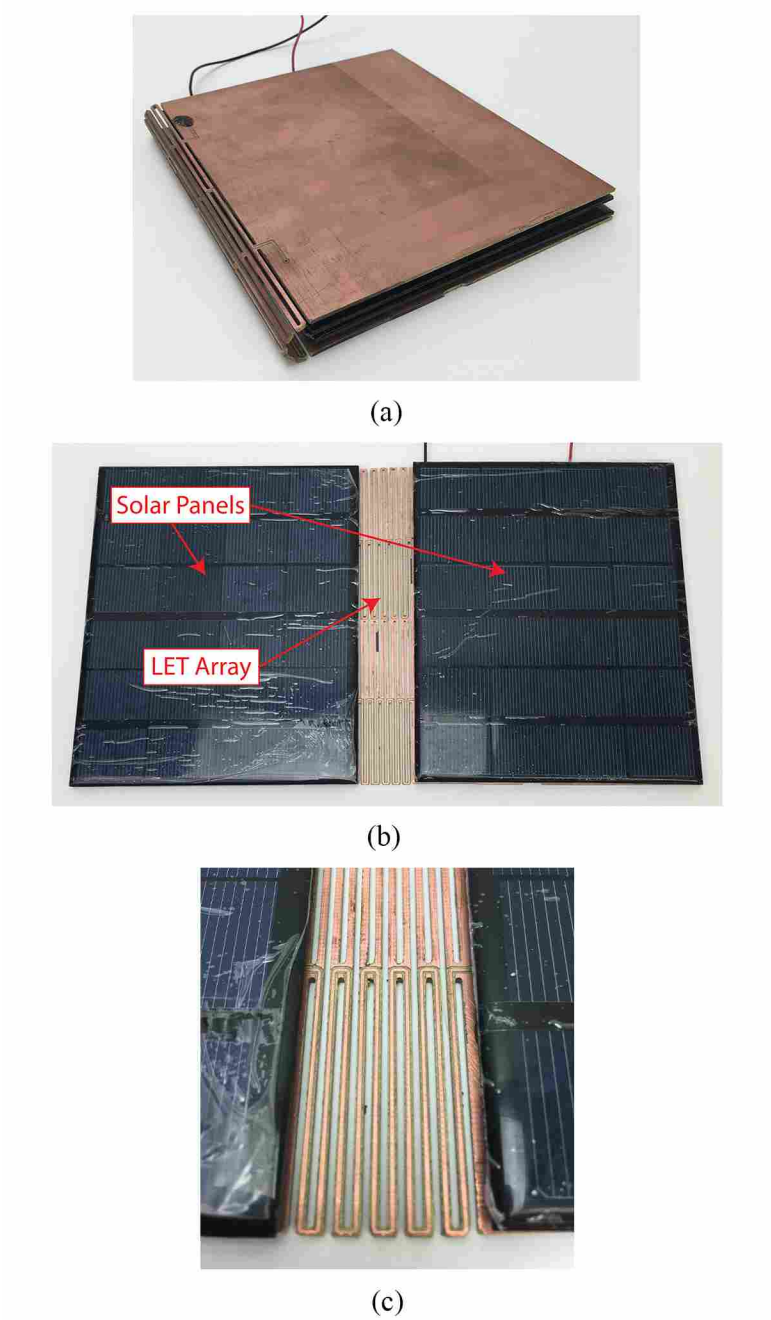


(a)

(b)

(c)

Figure 3.6: (a) Prototype solar array with LET joint hinge in folded and (b) unfolded configurations, along with (c) a detail view of the LET joint array surrogate hinge.

The hinge was designed using an array with 2 LET joints in parallel and 5 LET joints in series ($m = 2$, $n = 5$). The torsional members of each LET joint had a length of $l_t = 3.68$ cm and a width of $w_t = 0.13$ cm. The bending members of each LET joint had a length of $l_b = 0.38$ cm and a width of $w_b = 0.13$ cm. Overall, the hinge section was 15.24 cm along the bending axis and 2.16 cm perpendicular to the bending axis. A detail view of the LET joint array with exposed copper traces is shown in Fig. 3.6c.

The prototype demonstrated the ability to deflect 180° without mechanical failure or degradation of electrical performance.

### 3.3.3 Testing

To simulate repeated use of the device, a fatigue testing device was customized to accommodate the hinge portion of the prototype (see Fig. 3.7). Two copies of the hinge were produced and tested. On each hinge, two electrical traces were routed through the LET joints on the top, and two traces were routed through the LET joints on the bottom. A microcontroller (Arduino Uno with ATmega328P) was connected to each LET joint with a resistor in series and used as a voltage source and measurement device. The fatigue tester was used to deflect the board 180° at a rate of 20 cycles per minute. Voltage samples were taken at a rate of 140 samples per minute to detect if conductivity was lost.

The samples were deflected for 100,000 cycles. After the test, the samples were inspected for mechanical failure. The resistance of each trace across the hinge was also measured before and after testing. Resistance measurements are shown in Table 3.2.

As shown in Table 3.2, the resistance change of the traces was only 1.9% after 100,000 cycles. As no cracking or other mechanical failure of the traces was observed, this small increase in resistance is likely due to increased contact resistance from dust particles settling on the surface. These measurements show that there was no mechanical failure in any of the traces resulting from fatigue of the material.

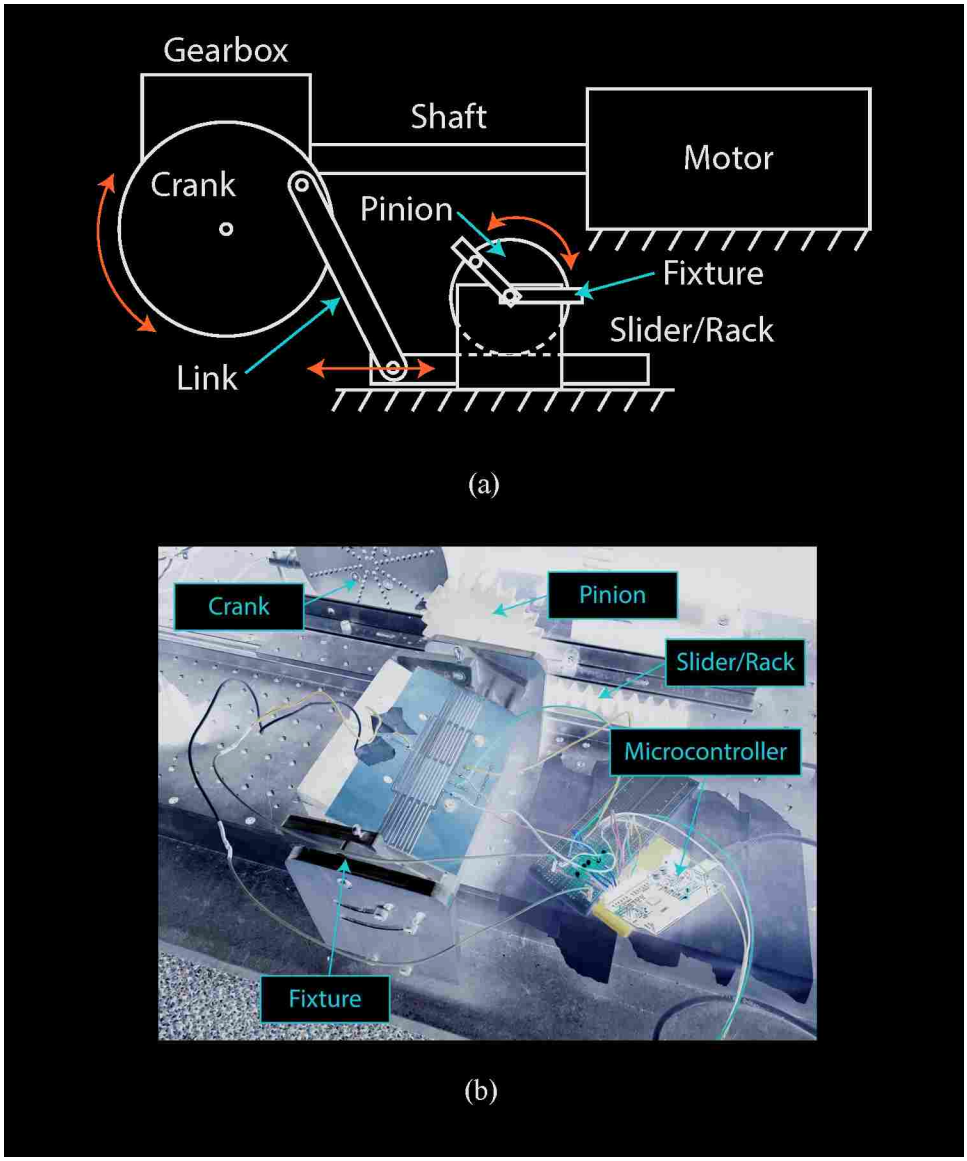


Figure 3.7: (a) Diagram and (b) photograph of fatigue testing setup.

### 3.3.4 Origami Map Fold

To demonstrate how this technique could be used to manufacture stowable PCBs, a prototype origami-like structure was designed and fabricated from a single sheet of copper-clad FR-4 fiberglass. An origami map fold [73] with two degree-four vertices [74] was selected.

Figure 3.8a shows the original origami fold pattern. Labels A, B, and C show the order of the folds. The structure is first folded in half on fold A. It is then folded in thirds on folds B and C. Figure 3.8b shows the regions where flexibility is to be added to facilitate folding. Figure 3.8c

Table 3.2: Resistance measurements of each trace on two boards before and after 100,000 cycles of 180 degree deflection. All values are in Ω. The small changes in resistance show that no mechanical failure occurred over the duration of the fatigue test.

| Trace | Resistance before test (Ω) | Resistance after test (Ω) | Change |
|---|---|---|---|
| Board 1 | | | |
| A | 0.412 | 0.417 | 1.4% |
| B | 0.431 | 0.442 | 2.6% |
| C | 0.422 | 0.425 | 0.8% |
| D | 0.413 | 0.437 | 5.8% |
| Board 2 | | | |
| A | 0.422 | 0.438 | 3.8% |
| B | 0.418 | 0.433 | 3.7% |
| C | 0.417 | 0.408 | -2.0% |
| D | 0.414 | 0.410 | -0.9% |
| Average change | | | 1.9% |

shows the surrogate hinge regions to be optimized. Labels $\alpha$, $\beta$, and $\gamma$ show the three separate optimization regions. When the structure is folded, $\alpha$ regions are folded first, so they should have a small bend radius when folded. $\beta$ and $\gamma$ regions are folded next, with $\gamma$ regions folded around $\beta$ regions. $\beta$ regions, then, should have a small bend radius, and $\gamma$ regions should have a larger bend radius to fold around the outside of the $\beta$ folds.

An optimization routine was employed to design the geometry of the surrogate hinge structures. Mixed integer programming was implemented using the APMonitor modeling language [75] and the IPOPT solver [76]. Structures $\alpha$, $\beta$, and $\gamma$ were each solved separately. Inside fold regions $\alpha$ and $\beta$ were optimized to minimize an objective function based on width of the fold while satisfying maximum Von Mises stress constraints. Outside fold region $\gamma$ was optimized to minimize Von Mises stress while satisfying geometric constraints which would allow the $\gamma$ folds to be folded around the $\beta$ folds.

The optimized dimensions for the $\alpha$ surrogate hinge were $w_t = 0.10$ cm, $l_t = 1.57$ cm, $w_b = 0.10$ cm, and $l_b = 0.10$ cm, with $m = 2$ members in parallel and $n = 6$ members in series. Dimensions for the $\beta$ hinge were $w_t = 0.10$ cm, $l_t = 1.93$ cm, $w_b = 0.10$ cm, and $l_b = 0.10$ cm,

with $m = 2$ members in parallel and $n = 5$ members in series. Dimensions for the $\gamma$ hinge were $w_t = 0.10$ cm, $l_t = 1.83$ cm, $w_b = 0.10$ cm, and $l_b = 0.10$ cm, with $m = 2$ members in parallel and $n = 15$ members in series. The thickness of the structure was 0.079 cm.

The entire structure was fabricated from a single sheet of material using a CNC mill. Figure 3.9 shows the fabricated structure being folded. In its folded state, the single PCB is folded into six stacked layers and the structure occupies approximately 17% of its original footprint.

This demonstrates the utility of this regional stiffness reduction technique in designing flexible PCBs that undergo complex kinematics and can be fabricated from a single sheet. This has the potential to reduce manufacturing complexity and costs for such devices. These devices could be folded to install or undergo repeated deflection in use, as shown above. In addition, the surrogate hinges provide structure to the mechanism that is not available using a polyimide substrate alone.

## 3.4 Conclusion

This chapter presents an approach using geometric features, such as LET arrays, to create regions of flexibility on a rigid printed circuit board. This creates regions of high stiffness to avoid putting high stress on components, while also having regions that exhibit high flexibility. It enables engineers to add flexibility to parts of PCB designs while avoiding the trade-offs that exist with global flexibility. The concept was demonstrated here using LET arrays, but other surrogate hinges could also be used.

Prototypes were designed, fabricated, and tested to verify the approach and models. LET-array surrogate hinges were the basis of the prototypes, and single hinges were constructed and tested. After 100,000 cycles of 180 degrees of angular deflection, the average resistance change was less than 2%. An origami-based design demonstrated an extreme example of multiple folds, resulting in a single sheet being folded into six stacked layers with about 17% of its original footprint.

This approach could be useful in applications where PCBs are desired to conform to an arbitrary shape (see Fig. 3.10). For example, boards could be folded for installation. Boards could be designed with multiple panels that could fit within some space or against the walls of a container. Circuit boards based on this design could be folded to save space in stowing and deployed for increased surface area during use.

This stiffness reduction technique also provides a way to have robustness in dynamic situations where the board is deflected and relaxed repeatedly. The surrogate hinge acts as both the electrical connection and the mechanical structure. This would increase simplicity and reduce cost. In addition, its monolithic design allows it to be manufactured at small or large scales.

This work shows that flexibility can be achieved in electronic circuits using geometric design. Such an approach is readily modeled and is manufacturable using current techniques. Using surrogate hinges to create regions of flexibility and rigidity opens new possibilities for designing flexible and conformable electronics.

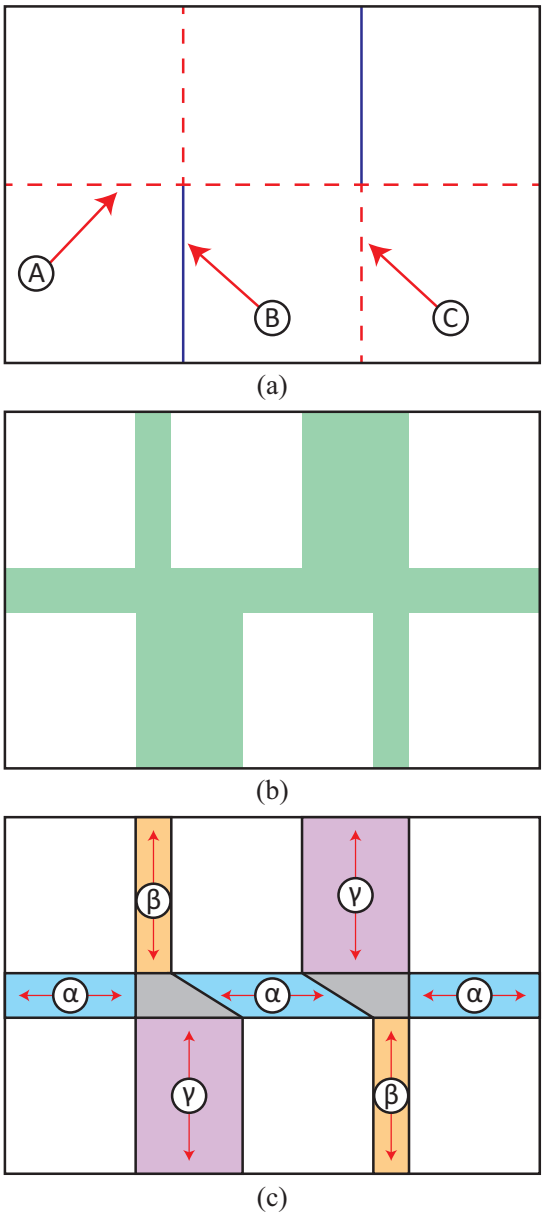


Figure 3.8: Map-fold origami pattern. (a) Origami fold pattern. Blue solid lines represent mountain folds, and red dashed lines represent valley folds. Labels A, B, and C designate the three folding steps in order of folding sequence. (b) The fold area to be made flexible with surrogate hinges is shown shaded in green. (c) Surrogate hinge areas are colored. Red arrows show the direction of the fold axis. Labels $\alpha$, $\beta$, and $\gamma$ designate regions of optimized surrogate fold geometry. Gray regions show areas where material is removed.

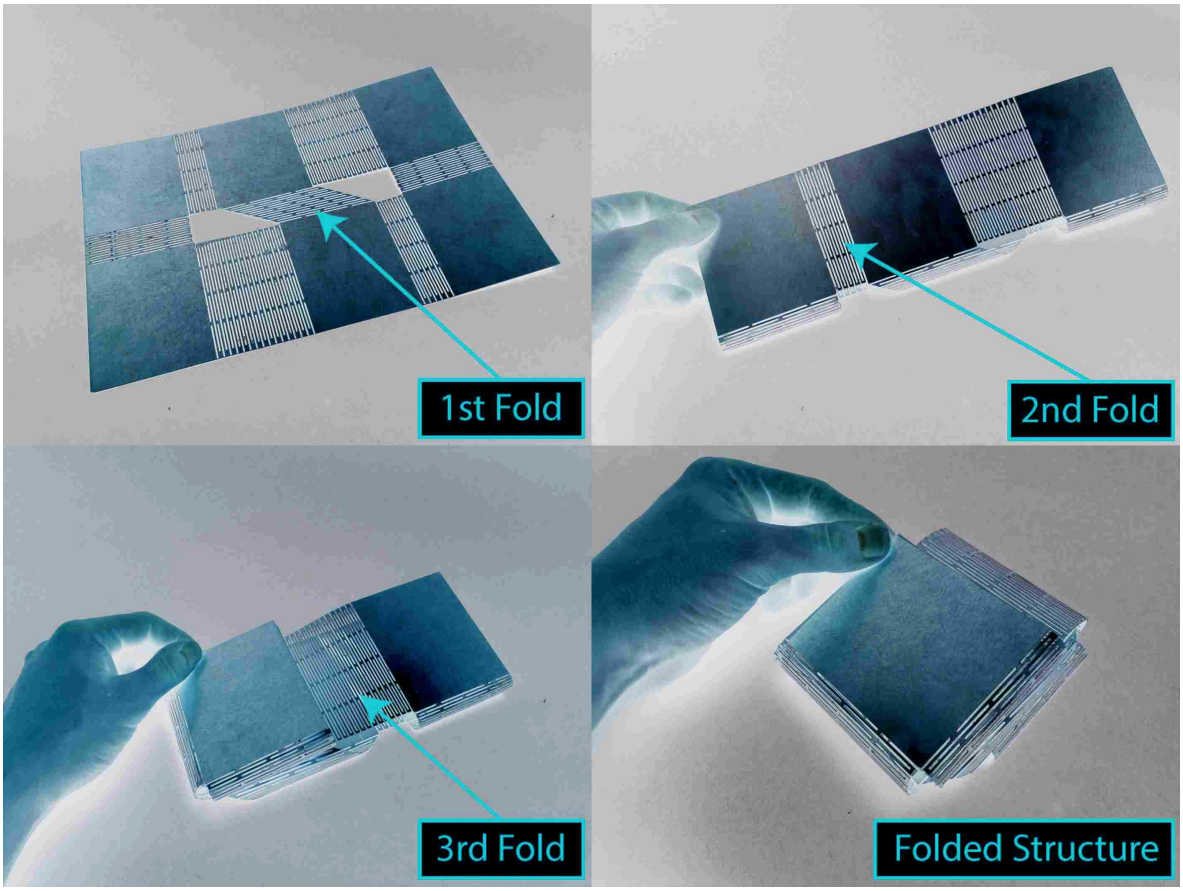


Figure 3.9: Origami-like folding structure designed with optimized surrogate hinge LET joint arrays and fabricated from a single sheet of copper-clad FR-4.

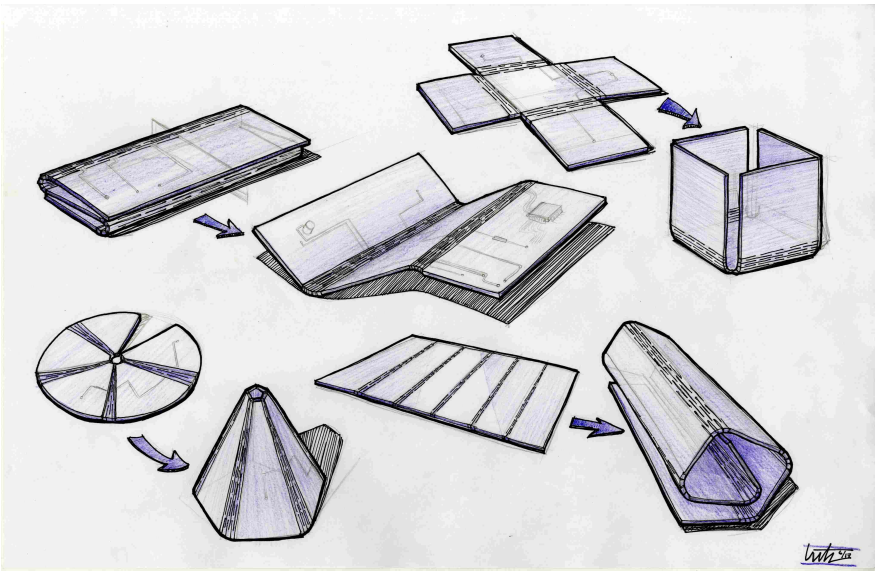

Figure 3.10: Possible form factors for various applications of this regional stiffness reduction technique. Circuit boards could be folded to stow in small spaces or to conform to an arbitrary shape.

# CHAPTER 4. OPTIMIZATION OF LET JOINT ARRAYS FOR USE AS SURROGATE HINGES IN MONOLITHIC THICK ORIGAMI

## 4.1 Introduction

Surrogate hinges enable designers to create monolithic bending structures fabricated from a single sheet of material. By reducing stiffness regionally, they can be used to mimic creases in origami patterns. This makes surrogate hinges a useful tool for origami-based design.

One geometric feature used for surrogate hinges is the LET joint [14]. LET joints can be arrayed in series and parallel (see Sec. 3.2.2). Arrays of LET joints enable significant reduction in stiffness. However, their many independent design variables make designing LET joint arrays a complex process (see Sec. 3.3.1).

This work presents an approach for optimizing LET joint array geometry based on an analytical model [14]. This approach uses the APMonitor modeling language [75] and the IPOPT solver [76]. The approach presented here was used to design the surrogate hinges in Sec. 3.3.4.

## 4.2 Background

Advances in computational power and methods have enabled optimization techniques to be used in increasingly complex structural design [77–80]. Optimization techniques have been used in the design of compliant mechanisms [81, 82]. These techniques lead to increased design performance and faster development times.

The selection of an optimization algorithm depends on the type of problem to be solved. Mixed-integer programming problems include both discrete and continuous design variables [83, 84]. These approaches are well-suited for optimizing LET joint arrays because designing LET arrays includes selecting dimensions (which are continuous variables) and the number of arrayed LET joints in parallel and series (which are discrete variables). The interior point solver IPOPT [76] is a robust solver that is capable of performing mixed-integer nonlinear programming. The

IPOPT solver has been used in such applications as valve optimization for water systems [85], muskuloskeletal modeling [86], and structural topology optimization [87]. Because of its robust performance and versatility, it is well-suited to optimize surrogate hinge geometry.

To aid in the development of optimization models, a modeling language may be used which formulates and manages the optimization problem and implements several solvers with a unified interface. The APMonitor modeling language [75] is a tool to perform modeling, optimization, estimation, and predictive control. It supports several solvers, including the interior point solver IPOPT [76] and the active set solver APOPT [88]. APMonitor facilitates rapid iteration of optimization problems by automating and abstracting problem setup. This makes it easier for designers to solve mixed-integer nonlinear optimization problems quickly compared to lower-level techniques which may require substantial refactoring when changing equations, objective functions, and constraints.

## 4.3 Approach

The APMonitor modeling language was used to set up the arrayed LET joint optimization problem. APMonitor offers several advantages over other systems. First, it provides access to high-performance solvers which are capable of solving mixed-integer nonlinear programming problems. Second, it automates equation, gradient, and constraint setup from the model the user inputs, simplifying the interface with the solvers and enabling quick switching between solvers. Third, it can optimize solving using remote access to high-performance computing resources. These advantages make it well-suited for designs that may need a high degree of iteration.

Because the model described below includes nonlinearity and mixed integers, the IPOPT solver was implemented in APMonitor to optimize the analytical model. The following sections describe the parameters (constants and variables), equations, objective functions, and constraints used in this optimization.

### 4.3.1 Constants

Several constants are used in the LET joint equations, as shown in Table 4.1. These constants are set in the .apm modeling file. They include material, geometric, and loading properties.

The modulus of elasticity ($E$) and Poisson's ratio ($\nu$) are properties of the selected material. The shear modulus ($G$) is a material property that can be calculated from $E$ and $\nu$ by

$$G = \frac{E}{2(1+\nu)} \tag{4.1}$$

The material thickness ($t$) is selected prior to the optimization and held constant in the optimization. The total desired deflection $\theta$ is also selected. This is the total angle the surrogate hinge should be able to deflect without failure.

Table 4.1: Constants in LET joint array optimization.

| Constants | | |
|---|---|---|
| Symbol | Name | Units |
| $E$ | Modulus of Elasticity | psi/Pascals |
| $G$ | Shear Modulus | psi/Pascals |
| $\nu$ | Poisson's Ratio | - |
| $t$ | Material Thickness | Inches/Centimeters |
| $\theta$ | Total Deflection | Radians |

### 4.3.2 Variables

Design variables selected by the optimizer are the geometric parameters of the LET joint array. These variables are shown in Fig. 4.1 and Table 4.2.

The variables $m$ and $n$ are used to designate the number of LET joints in parallel and series, respectively. The stiffness of the surrogate hinge and the moment induced by the applied angular displacement are directly proportional to $m$. However, the torsional and bending stresses of individual LET joints are inversely proportional to the number of LET joints in parallel $m$. Therefor, the total Von Mises stress is independent of the number of LET joints in parallel. Although LET joints in parallel do not affect the joint stress, they are useful in adding stability to the surrogate hinge. The stiffness of the surrogate hinge and the moment induced by the applied angular displacement are inversely proportional to the number of LET joints in series $n$, so adding more joints in series is useful in making the surrogate hinge more flexible.

The remaining design variables describe the geometry of the arrayed LET joints, where $w_i$ is the inner bending member width and $w_b$ is the outer bending member width. The length of the bending members is equal to the slot width $w_s$. The LET joint is designed to derive flexibility from its torsional members, so bending member geometry contributes less to the overall flexibility of the joint than does torsion member geometry. The width of the torsion members is $w_t$, and $l_t$ is the length of the torsion members.

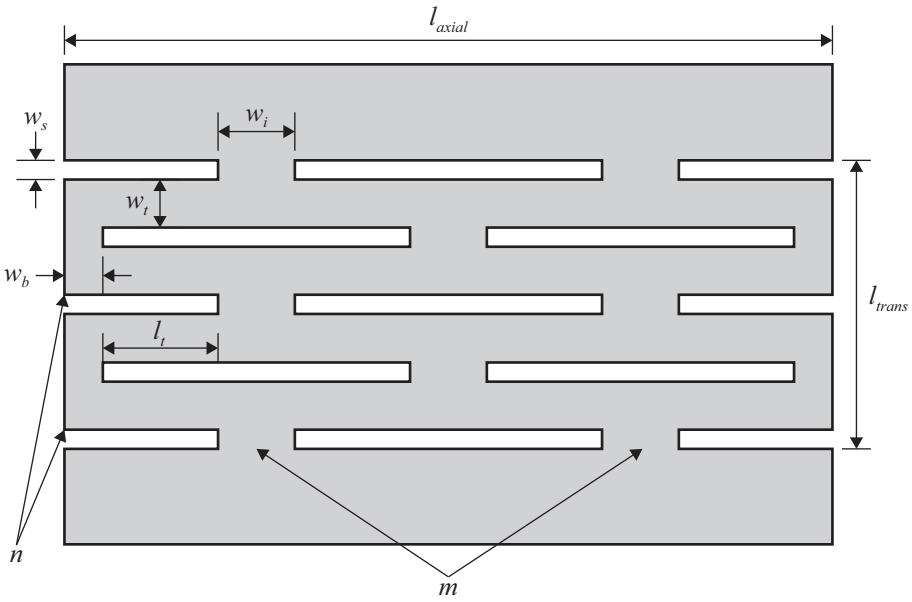


Figure 4.1: LET joint array with design variables labeled.

### 4.3.3 Equations

The APMonitor modeling language has the capability to handle intermediate equations when solving optimization problems. It is advantageous to include these equations in the model so that constraints and objective functions can be changed without refactoring the entire problem.

Two geometric relations are first established. The transverse length (perpendicular to the flexible axis) $l_i$ of an individual LET joint is given by

$$l_i = 2w_t + w_s \tag{4.2}$$

Table 4.2: LET joint array design variables to be optimized.

| Design Variables | | |
|---|---|---|
| Symbol | Name | Units |
| $m$ | LET Joints in Parallel | Integer |
| $n$ | LET Joints in Series | Integer |
| $w_i$ | Inner Bending Member Width | Inches/Centimeters |
| $w_b$ | Outer Bending Member Width | Inches/Centimeters |
| $w_t$ | Torsion Member Width | Inches/Centimeters |
| $l_t$ | Torsion Member Length | Inches/Centimeters |
| $w_s$ | Slot Width | Inches/Centimeters |
| $l_{axial}$ | Axial Length of Array | Inches/Centimeters |
| $l_{trans}$ | Transverse Length of Array | Inches/Centimeters |

The second moment of area $I_b$ of each bending member is

$$I_b = \frac{w_b t^3}{12} \tag{4.3}$$

Next, the stiffness of the LET joint array is calculated. The stiffness $k_b$ of each bending member is given by

$$k_b = \frac{E(\frac{w_b t^3}{12})}{l_i} \tag{4.4}$$

The stiffness $k_t$ of each torsion member is

$$k_t = \frac{K_i G}{l_t} \tag{4.5}$$

where $K_i$ is a geometry-dependent parameter approximated by Roark and Young [89] as

$$K_i = w_t t^3 \left[\frac{1}{3} - 0.21\frac{t}{w_t}\left(1 - \frac{t^4}{12w_t^4}\right)\right] \tag{4.6}$$

Combining the bending stiffness and torsional stiffness yields an overall stiffness $k_{unit}$ of an individual LET joint given by

$$k_{unit} = \frac{2k_b k_t}{k_t + 2k_b} \tag{4.7}$$

When LET joints are arrayed with $m$ joints in parallel and $n$ joints in series, the overall stiffness $k_{array}$ of the array in the transverse direction (perpendicular to the hinge axis) is

$$k_{array} = \frac{m}{n} k_{unit} \tag{4.8}$$

With the stiffness equations defined, the Von Mises stress can be calculated. When an angular displacement $\theta$ is applied to a surrogate hinge composed of an array of LET joints, a moment $M$ is induced in the array, which is

$$M = k_{array}\theta \tag{4.9}$$

The maximum torsional stress $\tau_{max}$ in each LET joint is

$$\tau_{max} = \frac{M}{2mQ} \tag{4.10}$$

where $Q$ is a geometry-dependent parameter, defined for a rectangular cross section by

$$Q = \frac{w_t^2 t^2}{3w_t + 1.8t} \tag{4.11}$$

The maximum bending stress $\sigma_{max}$ in each LET joint is

$$\sigma_{max} = \frac{Mt}{4mI_b} \tag{4.12}$$

Results from the above equations can be used in the equation for Von Mises stress $\sigma_{max,v}$, given by

$$\sigma_{max,v} = \sqrt{\sigma_{max}^2 + 3\tau_{max}^2} \tag{4.13}$$

Another component in the optimization of the surrogate hinge is the overall footprint of the LET joint array. The overall length of the array in the axial direction $l_{axial}$ (parallel to the hinge axis) is

$$l_{axial} = m(2w_b + 2l_t + w_i) \tag{4.14}$$

The overall length of the array in the transverse direction $l_{trans}$ (perpendicular to the hinge axis) is

$$l_{trans} = n(2w_s + 2w_t) + w_s \tag{4.15}$$

### 4.3.4 Objective Function and Constraints

Using the equations from Section 4.3.3, a designer has a variety of options to set up the optimization problem. Each uses a distinct objective function and set of constraints. We will focus on two scenarios: minimizing stress and minimizing footprint.

#### Minimize Stress

One approach to optimizing a LET joint array is to minimize the Von Mises stress of the LET joints while applying geometric constraints. This gives the optimizer a limit to the total size of footprint the surrogate hinge can occupy while designing geometry that produces the lowest possible stresses when deflected. The Von Mises stress of the optimized structure can be compared to the yield strength of the material to predict whether or not the design would be robust under the specified loading conditions.

Several constraints are necessary to ensure a feasible and manufacturable solution. $m$ and $n$ must be integers greater than or equal to 1. To increase stability, the designer may wish to set a lower bound of 2 for $m$ (LET joints in parallel). Lower bounds are also set for $w_i$, $w_b$, $w_t$, and $w_s$ to ensure robustness during fabrication and handling.

The size of the footprint is constrained by setting upper bounds for the parameters $l_{axial}$ and $l_{trans}$. The optimizer is set to minimize the Von Mises stress.

#### Minimize Footprint

Another approach to optimizing the LET joint array is to minimize the footprint the array occupies while applying a constraint on the Von Mises stress. A designer can use this approach to avoid failure in the joint under an applied angular deflection, while making the joint take up as little space as possible.

The same feasibility constraints are applied as in the stress minimization problem (lower bounds on $m$, $n$, $w_i$, $w_b$, $w_t$, and $w_s$). In addition, an upper bound is applied to $\sigma_{max,v}$. $l_{axial}$ or $l_{trans}$ may be minimized with a constraint placed on the dimension that is not minimized, or an objective function may be constructed which combines the two (e.g. minimize total area, which is the product of $l_{axial}$ and $l_{trans}$).

## 4.4 Results

The approach described in Sec. 4.3 was used to design the surrogate hinges in Sec. 3.3.4. A photograph of the fabricated structure with optimized surrogate hinges is shown in Fig. 4.2. Three different geometries of surrogate hinges were designed and are labeled in Fig. 4.2 as $\alpha$, $\beta$, and $\gamma$. The $\alpha$ and $\beta$ hinges were optimized to minimize footprint to have the smallest possible bend radius. The $\gamma$ hinge had to fold around the $\beta$ hinge, so it was optimized to minimize stress with a constrained footprint.

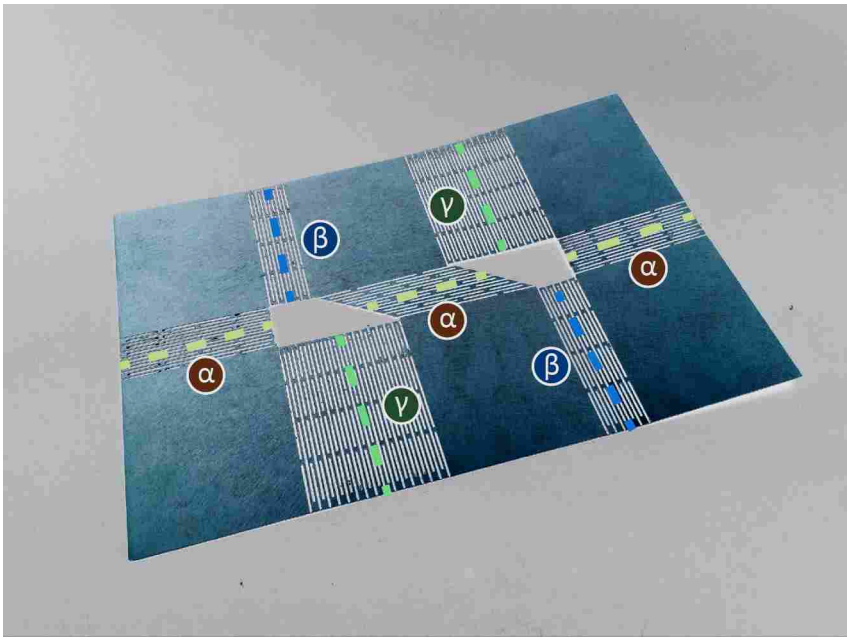


Figure 4.2: Monolithic map fold origami structure from Sec. 3.3.4. Regions $\alpha$, $\beta$, and $\gamma$ were optimized separately.

The results of the optimization are shown in Table 4.3. After the optimization, the structure was modified slightly to facilitate fabrication within the specified area. Table 4.3 shows the comparison between the optimized structure and the modified fabricated structure. This discrepancy could be avoided if a global optimizer were used which optimized all surrogate hinges simultaneously, rather than optimizing regions $\alpha$, $\beta$, and $\gamma$ separately.

The interior point solver converged on a solution for each hinge quickly. The $\alpha$ hinge converged in 8.10E-2 seconds with 188 nonlinear programming iterations. The $\beta$ hinge converged in 6.39E-2 seconds with 143 nonlinear programming iterations. The $\alpha$ hinge converged in 3.24E-2 seconds with 56 nonlinear programming iterations.

Table 4.3: Results from the LET joint array parameter optimization. $\alpha$, $\beta$, and $\gamma$ correspond to the surrogate hinges in Fig. 4.2. Columns labeled "Opt." correspond to optimization results. Columns labeled "Fab." correspond to the modified structure that was fabricated. Fabricated dimensions differ from optimized dimensions to facilitate the entire structure fitting in the given area.

| | $\alpha$ | | $\beta$ | | $\gamma$ | |
|---|---|---|---|---|---|---|
| Variable | Opt. | Fab. | Opt. | Fab. | Opt. | Fab. |
| $m$ | 2 | 2 | 2 | 2 | 2 | 2 |
| $n$ | 6 | 6 | 5 | 5 | 15 | 15 |
| $w_i$ (cm) | 0.28 | 0.20 | 0.20 | 0.20 | 0.20 | 0.20 |
| $w_b$ (cm) | 0.15 | 0.10 | 0.18 | 0.10 | 0.20 | 0.10 |
| $w_t$ (cm) | 0.10 | 0.10 | 0.10 | 0.10 | 0.10 | 0.10 |
| $l_t$ (cm) | 1.54 | 1.57 | 1.83 | 1.93 | 1.83 | 1.83 |
| $w_s$ (cm) | 0.10 | 0.10 | 0.10 | 0.10 | 0.10 | 0.10 |
| $l_{axial}$ (cm) | 7.39 | 7.11 | 8.53 | 8.53 | 8.53 | 8.53 |
| $l_{trans}$ (cm) | 2.54 | 2.54 | 2.13 | 2.13 | 6.40 | 6.20 |
| Stress (MPa) | 136.4 | 148.2 | 137.4 | 147.3 | 45.2 | 51.6 |

The structure shown in Fig. 4.2 was fabricated from a single sheet of FR-4 fiberglass using a CNC mill. It was able to undergo 180° of angular deflection without experiencing mechanical failure or yielding.

## 4.5 Conclusion

This work shows how mixed-integer nonlinear programming can be used to optimize LET joint arrays to be used as surrogate hinges. This helps designers overcome design complexity stemming from the high number of independent design variables in LET joint arrays. It also facilitates design based on material or space constraints. Optimization techniques assist designers in selecting feasible geometry for the design of surrogate hinges for origami applications.

This work demonstrates that this optimization approach can produce surrogate hinges that add regions of flexibility to rigid printed circuit board material. The optimized structure designed here was fabricated and shown to be able to undergo 180° of angular deflection without mechanical failure. This structure was fabricated from a single sheet of material. This shows that the optimization approach could be used to design monolithic origami-based structures from materials with high stiffness.

Future work could explore and compare various other optimization techniques, including topology optimization and gradient-free techniques. Other techniques could also be developed which optimize an entire origami structure simultaneously, rather than solving each hinge individually.

# CHAPTER 5. CONCLUSION

## 5.1 Summary

As research continues to advance origami-based engineering, new avenues are opening for mechanism design. This work introduced several of these new channels.

A new type of mechanism was introduced and called "conceal-and-reveal." These mechanisms cover or protect (conceal) and uncover or expose (reveal) a payload. A method of developing conceal-and-reveal mechanisms was developed. Example mechanisms were developed using this method. This method could be applied to develop other conceal-and-reveal mechanisms for different applications. It is also general enough to be applicable to other applications of thick-origami design.

A technique for regional stiffness reduction in printed circuit boards (PCBs) using lamina emergent torsional (LET) joints was also presented. Analytical and finite element models were developed to design and analyze PCBs using this method. A design was prototyped and was shown to be robust over a long life through fatigue testing. A prototype of an origami-based structure was also constructed using this technique. An optimization method was developed to support the regional stiffness reduction technique and was used to design the origami-based structure.

The methods presented in this research open new avenues for origami-based engineering design. They also give designers new tools for developing origami-based mechanisms. Methods such as these will be valuable as origami becomes the basis for more engineered systems in the future.

## 5.2 Limitations

The work in this thesis has several limitations. The method for designing thick-origami systems outlined in Chapter 2 can be generalized to thick-origami-adapted systems, but is not

well-suited for designing origami-inspired systems (which do not exhibit the same kinematics of true origami patterns) or systems with near-zero thickness (which do not require thickness accommodation). In addition, the conceal-and-reveal definition presented in this work is a broad classification of a function that engineered systems may exhibit, but it is not a prescription of a specific motion.

The stiffness reduction technique for printed circuit boards has only been tested for PCBs on the order of a few square centimeters of footprint. Sizes much smaller or larger were not tested. The resistance measurements before and after the fatigue test show that the structure did not fail mechanically, but could be repeated more thoroughly. Leads could be soldered directly onto the traces to eliminate surface resistance and make measurements more reliable. More samples could also be tested. Samples could be tested for strength and fatigue under multiple different loading conditions (tension, compression, etc.).

The optimization approach could also be further studied. Since each surrogate hinge was optimized separately, the overall structure is likely not the global optimum. In addition, multiple geometries of surrogate hinge (besides the LET joint) could be considered in the optimization, and other loading conditions could be considered in the objective function and constraints. Thus, we cannot say that the example structures shown here are the complete optimum structures.

## 5.3 Conclusions

Origami-adapted design is a broad category of systems that engineers can design for. This work shows that structured approaches can be useful in developing new avenues for origami design. The techniques discussed here could be useful in a variety of applications, and the general approaches outlined here can be used for various design problems.

This work also shows that it is possible to produce robust flexible printed circuit boards using principles of compliant mechanisms. These PCBs could be made less expensively than polyimide/fiberglass hybrid PCBs and could have regions of stiffness and islands of rigidity. This opens new possibilities for flexible and conformal electronics.

## 5.4 Future Work

Further work can be done to apply the ideas developed in this research. More classes of origami-based mechanisms could be developed and defined, similar to how the conceal-and-reveal motion is introduced here. Origami-based mechanisms could be particularly useful in applications that require the motion of panels or that require compact and expanded configurations.

More work could also be done to develop optimization techniques for the stiffness reduction technique presented here. Topology optimization and gradient-free methods could be explored and compared. A method could be developed to optimize an entire origami structure at once, with all surrogate hinges being considered simultaneously.

Further applications for the technologies presented here could be explored. Conceal-and-reveal mechanisms could be used in the design of applications such as:

- Clandestine systems that require a payload that must be shielded from detection until use
- Scientific instruments that must be protected from harsh environments until deployment
- Space systems that must be protected during launch and deployed at a later time
- Fragile products such as chemical containers that must be protected during transportation
- Containers of many small components that must remain organized during storage and use

The stiffness-reduction method using surrogate hinges could be used for applications such as:

- Increasing the robustness of folding consumer electronics devices such as backpackable solar chargers
- Manufacturing space-deployed solar structures such as the origami flasher described by Zirbel [1]
- Reducing the manufacturing complexity and cost of existing flexible electronic systems
- Reducing stresses due to mechanical strain on electronic components in flexible electronic systems
- Reducing stresses due to impact in rigid electronic systems

- Designing origami structures on the micro-scale

These technologies could also be applied to humanitarian design or design for the developing world. Examples could include:

- Conceal-and-reveal packaging of medical equipment for protection in harsh environments and quick, easy access
- Deployable shelters designed using thick origami methods
- Portable, collapsible furniture for use by refugees
- Portable, folding solar panel arrays to provide electricity and lighting
- Inexpensive, durable consumer electronics products with folding components

## REFERENCES


[1] Zirbel, S. A., Lang, R. J., Thomson, M. W., Sigel, D. A., Walkemeyer, P. E., Trease, B. P., Magleby, S. P., and Howell, L. L., 2013. "Accommodating thickness in origami-based deployable arrays." *Journal of Mechanical Design,* **135**(11), p. 111005. 1, 2, 5, 6, 11, 25, 58

[2] Tachi, T., 2011. "Rigid-foldable thick origami." In *Origami 5: Fifth International Meeting of Origami Science, Mathematics, and Education*, P. Wang-Iverson, R. Lang, and M. Yim, eds., CRC Press, pp. 253–264. 1, 6, 8, 11, 18, 24

[3] Hoberman, C., 1991. Reversibly expandable structures US Patent 4,981,732. 1, 6, 11

[4] Hoberman, C., 2010. Folding structures made of thick hinged sheets US Patent 7,794,019. 1, 6, 11

[5] Abel, Z., Cantarella, J., Demaine, E. D., Eppstein, D., Hull, T. C., Ku, J. S., Lang, R. J., and Tachi, T., 2016. "Rigid Origami Vertices: Conditions and Forcing Sets." *Journal of Computational Geometry,* **7**(1), pp. 171–184. 1, 6, 11

[6] Chen, Y., Peng, R., and You, Z., 2015. "Origami of thick panels." *Science,* **349**(6246), pp. 396–400. 1, 6, 11, 18

[7] Edmondson, B. J., Lang, R. J., Magleby, S. P., and Howell, L. L., 2014. "An offset panel technique for thick rigidily foldable origami." In *ASME 2014 International Design Engineering Technical Conferences and Computers and Information in Engineering Conference*, American Society of Mechanical Engineers, pp. V05BT08A054–V05BT08A054. 1, 6, 11, 14

[8] Delimont, I. L., Magleby, S. P., and Howell, L. L., 2015. "A family of dual-segment compliant joints suitable for use as surrogate folds." *Journal of Mechanical Design,* **137**(9), p. 092302. 1, 30

[9] Delimont, I. L., Magleby, S. P., and Howell, L. L., 2015. "Evaluating compliant hinge geometries for origami-inspired mechanisms." *Journal of Mechanisms and Robotics,* **7**(1), p. 011009. 1, 30

[10] Morgan, J., 2015. "An approach for designing origami-adapted products with aerospace mechanism examples." Master's thesis, Brigham Young University. 2

[11] Harris, K., Elias, A., and Chung, H.-J., 2016. "Flexible electronics under strain: a review of mechanical characterization and durability enhancement strategies." *Journal of Materials Science,* **51**(6), pp. 2771–2805. 2, 28, 29

[12] Wang, J., Sugimura, Y., Evans, A., and Tredway, W., 1998. "The mechanical performance of dlc films on steel substrates." *Thin Solid Films,* **325**(1), pp. 163–174. 2, 29

[13] Lewis, J., 2006. "Material challenge for flexible organic devices." *Materials today,* **9**(4), pp. 38–45. 2, 29

[14] Jacobsen, J. O., Chen, G., Howell, L. L., and Magleby, S. P., 2009. "Lamina Emergent Torsional (LET) Joint." *Mechanism and Machine Theory,* **44**(11), Nov, pp. 2098–2109. 3, 30, 31, 46

[15] Filipov, E. T., Tachi, T., and Paulino, G. H., 2015. "Origami tubes assembled into stiff, yet reconfigurable structures and metamaterials." *Proceedings of the National Academy of Sciences,* **112**(40), pp. 12321–12326. 4

[16] Shaar, N. S., Barbastathis, G., and Livermore, C., 2015. "Integrated folding, alignment, and latching for reconfigurable origami microelectromechanical systems." *Journal of Microelectromechanical Systems,* **24**(4), pp. 1043–1051. 4

[17] Silverberg, J. L., Evans, A. A., McLeod, L., Hayward, R. C., Hull, T., Santangelo, C. D., and Cohen, I., 2014. "Using origami design principles to fold reprogrammable mechanical metamaterials." *Science,* **345**(6197), pp. 647–650. 4

[18] Han, D., Pal, S., Nangreave, J., Deng, Z., Liu, Y., and Yan, H., 2011. "Dna origami with complex curvatures in three-dimensional space." *Science,* **332**(6027), pp. 342–346. 4

[19] Wang, F., Gong, H., Chen, X., and Chen, C., 2016. "Folding to curved surfaces: A generalized design method and mechanics of origami-based cylindrical structures." *Scientific Reports,* **6**, p. 33312. 4

[20] Ku, J. S., and Demaine, E. D., 2016. "Folding flat crease patterns with thick materials." *Journal of Mechanisms and Robotics,* **8**(3), p. 031003. 5

[21] Francis, K. C., Rupert, L. T., Lang, R. J., Morgan, D. C., Magleby, S. P., and Howell, L. L., 2014. "From crease pattern to product: Considerations to engineering origami-adapted designs." In *ASME 2014 International Design Engineering Technical Conferences and Computers and Information in Engineering Conference*, American Society of Mechanical Engineers, pp. V05BT08A030–V05BT08A030. 5

[22] Reynolds, W. D., Jeon, S. K., Banik, J. A., and Murphey, T. W., 2013. "Advanced folding approaches for deployable spacecraft payloads." In *ASME 2013 International Design Engineering Technical Conferences and Computers and Information in Engineering Conference*, American Society of Mechanical Engineers, pp. V06BT07A043–V06BT07A043. 5

[23] Butler, J., Morgan, J., Pehrson, N., Tolman, K., Bateman, T., Magleby, S. P., and Howell, L. L., 2016. "Highly compressible origami bellows for harsh environments." In *ASME 2016 International Design Engineering Technical Conferences and Computers and Information in Engineering Conference*, American Society of Mechanical Engineers, pp. V05BT07A001–V05BT07A001. 5

[24] Bruton, J. T., Nelson, T. G., Zimmerman, T. K., Fernelius, J. D., Magleby, S. P., and Howell, L. L., 2016. "Packing and deploying soft origami to and from cylindrical volumes with application to automotive airbags." *Royal Society Open Science,* **3**(9), p. 160429. 5

[25] Gioia, F., Dureisseix, D., Motro, R., and Maurin, B., 2012. "Design and analysis of a foldable/unfoldable corrugated architectural curved envelop." *Journal of Mechanical Design,* **134**(3), p. 031003. 5

[26] Miura, K., 1989. "A note on intrinsic geometry of origami." *Research of Pattern Formation, KTK Scientific Publishers, Tokyo, Japan*, pp. 91–102. 5

[27] Greenberg, H. C., Gong, M. L., Magleby, S. P., and Howell, L. L., 2011. "Identifying links between origami and compliant mechanisms." *Mechanical Sciences,* **2**(2), pp. 217–225. 5

[28] Lang, R. J., 2011. *Origami Design Secrets: Mathematical Methods for an Ancient Art*. A K Peters/CRC Press. 5, 9

[29] Bowen, L. A., Grames, C. L., Magleby, S. P., Howell, L. L., and Lang, R. J., 2013. "A Classification of Action Origami as Systems of Spherical Mechanisms." *Journal of Mechanical Design,* **135**(11, SI), NOV. 5

[30] Lang, R., 1996. "A computational algorithm for origami design." In *Proceedings of the twelfth annual symposium on Computational geometry*, ACM, pp. 98–105. 5

[31] Tachi, T., 2010. "Origamizing polyhedral surfaces." *IEEE transactions on visualization and computer graphics,* **16**(2), pp. 298–311. 5

[32] Tachi, T., 2013. "Designing freeform origami tessellations by generalizing resch's patterns." *Journal of Mechanical Design,* **135**(11), p. 111006. 5

[33] Evans, T. A., Lang, R. J., Magleby, S. P., and Howell, L. L., 2015. "Rigidly foldable origami gadgets and tessellations." *Royal Society Open Science,* **2**(9), SEP. 6, 9, 23

[34] Huffman, D. A., 1976. "Curvature and creases: A primer on paper." *IEEE Transactions on Computers,* **C-25**, pp. 1010 – 1019. 6

[35] Wu, W., and You, Z., 2010. "Modeling rigid origami with quaternions and dual quaternions." *The Royal Society,* **466**, pp. 2155–2174. 6

[36] Wang, K., and Chen, Y., 2011. "Folding a patterned cylinder by rigid origami." In *Origami 5: Fifth International Meeting of Origami Science, Mathematics, and Education*, P. Wang-Iverson, R. Lang, and M. Yim, eds., CRC Press, pp. 265–276. 6

[37] Tachi, T., 2009. "Generalization of rigid-foldable quadrilateral-mesh origami." *Journal of the International Association for Shell and Spatial Structures,* **50**(3), pp. 173–179. 6

[38] Evans, T. A., Lang, R. J., Magleby, S. P., and Howell, L. L., 2015. "Rigidly foldable origami twists." *Origami 6*, pp. 119–130. 6, 13, 17

[39] Morgan, M. R., Lang, R. J., Magleby, S. P., and Howell, L. L., 2016. "Towards developing product applications of thick origami using the offset panel technique." *Mechanical Sciences,* **7**(1), pp. 69–77. 6, 11, 13, 14

[40] Kusiak, A., and Wang, J., 1993. "Decomposition of the Design Process." *Journal of Mechanical Design,* **115**(4), DEC, pp. 687–695. 7

[41] Morgan, J., Magleby, S. P., Lang, R. J., and Howell, L. L., 2015. "A preliminary process for origami-adapted design." In *Proceedings of the ASME International Design Engineering Technical Conferences*, ASME DETC2015-47559. 7

[42] Helms, M., Vattam, S. S., and Goel, A. K., 2009. "Biologically inspired design: process and products." *Design Studies,* **30**(5), SEP, pp. 606–622. 7

[43] Morgan, J., Magleby, S. P., and Howell, L. L., 2016. "An Approach to Designing Origami-Adapted Aerospace Mechanisms." *Journal of Mechanical Design,* **138**(5), May. 7

[44] Watanabe, N., and Kawaguchi, K.-i., 2009. "The method for judging rigid foldability." *Origami,* **4**, pp. 165–174. 8

[45] Tachi, T., 2010. "Geometric considerations for the design of rigid origami structures." *Proceedings of the International Association for Shell and Spatial Structures (IASS) Symposium,* **12**(10), pp. 458–460. 8

[46] Schenk, M., Viquerat, A. D., Seffen, K. A., and Guest, S. D., 2014. "Review of inflatable booms for deployable space structures: packing and rigidization." *Journal of Spacecraft and Rockets*. 8

[47] Mattson, C. A., and Sorensen, C. D., 2013. *Fundamentals of Product Development*. Brigham Young University. 8

[48] Wang-Iverson, P., Lang, R. J., and Yim, M., 2016. *Origami 5: Fifth International Meeting of Origami Science, Mathematics, and Education*. CRC Press. 9

[49] Miura, K., Kawaskai, T., Tachi, T., Uehara, R., and Lang, R. J., 2016. *Origami 6: Sixth International Meeting of Origami Science, Mathematics, and Education*. American Mathematical Society. 9

[50] Fuchi, K., Buskohl, P. R., Bazzan, G., Durstock, M. F., Reich, G. W., Vaia, R. A., and Joo, J. J., 2015. "Origami actuator design and networking through crease topology optimization." *Journal of Mechanical Design,* **137**(9), p. 091401. 10

[51] Chen, G., Zhang, S., and Li, G., 2013. "Multistable behaviors of compliant sarrus mechanisms." *Journal of Mechanisms and Robotics,* **5**(2), p. 021005. 17

[52] Yoshimura, Y., 1955. "On the mechanism of buckling of a circular cylindrical shell under axial compression." *NACA TM 1390*. 23

[53] Miura, K., 1969. "Proposition of pseudo-cylindrical concave polyhedral shells." *ISAS report,* **34**(9), Nov, pp. 141–163. 23

[54] Norton, R. L., 2011. *Design of Machinery: An Introduction to the Synthesis and Analysis of Mechanisms and Machines*., 5 ed. McGraw-Hill. 25

[55] Borgesen, P., et al., 2016. "Effects of strain rate and amplitude variations on solder joint fatigue life in isothermal cycling." *Journal of Electronic Packaging,* **138**(2), p. 021002. 28

[56] Howell, L. L., 2001. *Compliant Mechanisms*. John Wiley & Sons, Inc., New York, NY. 28

[57] Weight, B. L., Mattson, C. A., Magleby, S. P., and Howell, L. L., 2007. "Configuration selection, modeling, and preliminary testing in support of constant force electrical connectors." *Journal of Electronic Packaging,* **129**(3), pp. 236–246. 28

[58] Chen, W., Bhat, A., and Sitaraman, S. K., 2015. "Impact isolation through the use of compliant interconnects for microelectronic packages." *Journal of Electronic Packaging,* **137**(4), p. 041005. 28

[59] Park, S., Vosguerichian, M., and Bao, Z., 2013. "A review of fabrication and applications of carbon nanotube film-based flexible electronics." *Nanoscale,* **5**(5), pp. 1727–1752. 29

[60] Zhu, S., So, J.-H., Mays, R., Desai, S., Barnes, W. R., Pourdeyhimi, B., and Dickey, M. D., 2013. "Ultrastretchable fibers with metallic conductivity using a liquid metal alloy core." *Advanced Functional Materials,* **23**(18), pp. 2308–2314. 29

[61] Yao, S., and Zhu, Y., 2015. "Nanomaterial-enabled stretchable conductors: strategies, materials and devices." *Advanced Materials,* **27**(9), pp. 1480–1511. 29

[62] Benight, S. J., Wang, C., Tok, J. B., and Bao, Z., 2013. "Stretchable and self-healing polymers and devices for electronic skin." *Progress in Polymer Science,* **38**(12), pp. 1961–1977. 29

[63] Sun, D.-M., Liu, C., Ren, W.-C., and Cheng, H.-M., 2013. "A review of carbon nanotube-and graphene-based flexible thin-film transistors." *Small,* **9**(8), pp. 1188–1205. 29

[64] Lipomi, D. J., and Bao, Z., 2011. "Stretchable, elastic materials and devices for solar energy conversion." *Energy & Environmental Science,* **4**(9), pp. 3314–3328. 29

[65] Zardetto, V., Brown, T. M., Reale, A., and Di Carlo, A., 2011. "Substrates for flexible electronics: A practical investigation on the electrical, film flexibility, optical, temperature, and solvent resistance properties." *Journal of Polymer Science Part B: Polymer Physics,* **49**(9), pp. 638–648. 29

[66] Zeng, W., Shu, L., Li, Q., Chen, S., Wang, F., and Tao, X.-M., 2014. "Fiber-based wearable electronics: A review of materials, fabrication, devices, and applications." *Advanced Materials,* **26**(31), pp. 5310–5336. 29

[67] Leterrier, Y., Medico, L., Demarco, F., Månson, J.-A., Betz, U., Escola, M., Olsson, M. K., and Atamny, F., 2004. "Mechanical integrity of transparent conductive oxide films for flexible polymer-based displays." *Thin Solid Films,* **460**(1), pp. 156–166. 29

[68] Vella, D., Bico, J., Boudaoud, A., Roman, B., and Reis, P. M., 2009. "The macroscopic delamination of thin films from elastic substrates." *Proceedings of the National Academy of Sciences,* **106**(27), pp. 10901–10906. 29

[69] Kim, S.-R., and Nairn, J. A., 2000. "Fracture mechanics analysis of coating/substrate systems: Part i: Analysis of tensile and bending experiments." *Engineering Fracture Mechanics,* **65**(5), pp. 573–593. 29

[70] Martynenko, E., Zhou, W., Chudnovsky, A., Li, R., and Poglitsch, L., 2002. "High cycle fatigue resistance and reliability assessment of flexible printed circuitry." *Journal of Electronic Packaging,* **124**(3), SEP, pp. 254–259. 29

[71] Karjalainen, P. H., and Heino, P., 2007. "On-wafer capacitors under mechanical stress." *Journal of Electronic Packaging,* **129**(3), SEP, pp. 287–290. 29

[72] Jacobsen, J. O., Winder, B. G., Howell, L. L., and Magleby, S. P., 2010. "Lamina Emergent Mechanisms and Their Basic Elements." *Journal of Mechanisms and Robotics - Transactions of the ASME,* **2**(1), Feb. 30

[73] Miura, K., 1980. "Method of packaging and deployment of large membranes in space." *Proceedings of 31st Congress International Astronautical Federation*, pp. 1–10. 39

[74] Waitukaitis, S., and van Hecke, M., 2016. "Origami building blocks: Generic and special four-vertices." *Physical Review E,* **93**(2), p. 023003. 39

[75] Hedengren, J. D., Shishavan, R. A., Powell, K. M., and Edgar, T. F., 2014. "Nonlinear modeling, estimation and predictive control in APMonitor." *Computers & Chemical Engineering,* **70**, pp. 133 – 148 Manfred Morari Special Issue. 40, 46, 47

[76] Wächter, A., and Biegler, L. T., 2006. "On the implementation of an interior-point filter line-search algorithm for large-scale nonlinear programming." *Mathematical Programming,* **106**(1), pp. 25–57. 40, 46, 47

[77] Haftka, R. T., and Grandhi, R. V., 1986. "Structural shape optimization a survey." *Computer Methods in Applied Mechanics and Engineering,* **57**(1), pp. 91–106. 46

[78] Bendsøe, M. P., and Kikuchi, N., 1988. "Generating optimal topologies in structural design using a homogenization method." *Computer Methods in Applied Mechanics and Engineering,* **71**(2), pp. 197–224. 46

[79] Wall, W. A., Frenzel, M. A., and Cyron, C., 2008. "Isogeometric structural shape optimization." *Computer Methods in Applied Mechanics and Engineering,* **197**(33), pp. 2976–2988. 46

[80] Munk, D. J., Vio, G. A., and Steven, G. P., 2015. "Topology and shape optimization methods using evolutionary algorithms: a review." *Structural and Multidisciplinary Optimization,* **52**(3), pp. 613–631. 46

[81] Frecker, M., Ananthasuresh, G., Nishiwaki, S., Kikuchi, N., and Kota, S., 1997. "Topological synthesis of compliant mechanisms using multi-criteria optimization." *Journal of Mechanical Design,* **119**(2), pp. 238–245. 46

[82] Hull, P. V., and Canfield, S., 2006. "Optimal synthesis of compliant mechanisms using subdivision and commercial fea." *Journal of Mechanical Design,* **128**(2), pp. 337–348. 46

[83] Grossmann, I. E., 2002. "Review of nonlinear mixed-integer and disjunctive programming techniques." *Optimization and Engineering,* **3**(3), pp. 227–252. 46

[84] Tawarmalani, M., and Sahinidis, N. V., 2004. "Global optimization of mixed-integer nonlinear programs: A theoretical and computational study." *Mathematical Programming,* **99**(3), pp. 563–591. 46

[85] Ghaddar, B., Claeys, M., Mevissen, M., and Eck, B. J., 2017. "Polynomial optimization for water networks: Global solutions for the valve setting problem." *European Journal of Operational Research,* **261**(2), pp. 450–459. 47

[86] Lee, L.-F., and Umberger, B. R., 2016. "Generating optimal control simulations of musculoskeletal movement using opensim and matlab." *PeerJ,* **4**, p. e1638. 47

[87] Rojas-Labanda, S., and Stolpe, M., 2015. "Benchmarking optimization solvers for structural topology optimization." *Structural and Multidisciplinary Optimization,* **52**(3), pp. 527–547. 47

[88] Hedengren, J., Mojica, J., Cole, W., and Edgar, T., 2012. "Apopt: Minlp solver for differential and algebraic systems with benchmark testing." In *Proceedings of the INFORMS National Meeting, Phoenix, AZ, USA*, Vol. 1417. 47

[89] Young, W. C., and Budynas, R. G., 2002. *Roark's Formulas for Stress and Strain.*, Vol. 7 McGraw-Hill New York. 50